State-of-the-Art Review

Scale of Fluctuation for Spatially Varying Soils: Estimation Methods and Values

Brigid Cami[1]; Sina Javankhoshdel, Aff.M.ASCE[2]; Kok-Kwang Phoon, F.ASCE[3]; and Jianye Ching, M.ASCE[4]

Abstract: Spatial variability is one of the major sources of uncertainty in geotechnical applications. This variability is characterized customarily by the scale of fluctuation. Scale of fluctuation describes the distance over which the parameters of a soil or rock are similar or correlated. The scale of fluctuation is required in order to best characterize and to simulate a spatially variable field. This paper first provides an overview of the various methods available for estimating the scale of fluctuation from cone penetration test (CPT) data, along with two examples for comparing the methods. The first part reveals some issues with two popular estimation methods, namely the method of moments and the maximum-likelihood method (MLE). The method of moments is less sensitive to the choice of the autocorrelation function (ACF), but it could be less precise and may be based on a correlation estimator that does not produce a positive definite autocorrelation matrix. MLE can be very sensitive to the choice of the classical one-parameter ACF. It is not uncommon to assume such an ACF, rather than to identify the ACF from actual soil data with a more general two-parameter Whittle–Matérn (WM) model. This practice may not be robust. Nonetheless, a literature survey is useful if these caveats are kept in mind. The second part of this paper provides a database table of horizontal and vertical scale of fluctuation values in different locations and for different materials, collected from published case studies, which can be used as a reference when field data are not readily available. The probable range of values as a function of soil type is provided to inform sensitivity analysis and to guide the selection of a prior distribution for Bayesian analysis. **DOI: 10.1061/AJRUA6.0001083.**

Introduction

Spatial variability is one of the major sources of uncertainty in geotechnical applications. In recent decades the necessity of considering spatial variability in geotechnical applications has been demonstrated in many studies (e.g., Griffiths and Fenton 1993; Griffiths 2009; Cho 2010; Soubra and Massih 2010; Hicks and Spencer 2010; Huang et al. 2010, 2013; Stuedlein et al. 2012; Cassidy et al. 2013; Jha and Ching 2013; Javankhoshdel and Bathurst 2014; Jiang et al. 2014; Le 2014; Li et al. 2015a; Javankhoshdel 2016; Xiao et al. 2016; Li et al. 2016; Luo et al. 2016; Javankhoshdel et al. 2017; Papaioannou and Straub 2017). The state of the practice is to characterize this spatial variability using the scale of fluctuation (θ). The scale of fluctuation describes the distance over which the parameters of a soil or rock are similar or correlated; soil properties sampled from adjacent locations in the soil profile tend to have similar values, and as the sampling distance increases the correlation decreases. The scale of fluctuation is possibly the minimum information needed to simulate a spatially variable field that bears some semblance to reality. It is used as an input to an autocorrelation function (ACF) model (e.g., Markovian or Gaussian), which is either prescribed or identified from empirical autocorrelation values at discrete lags through some fitting procedures. This ACF model defines the correlation between two points separated by any arbitrary interval and orientation [for two-dimensional (2D) and three-dimensional (3D) fields]. The scale of fluctuation by itself is insufficient—it can be viewed as a coarse descriptor of the spatial correlation structure in this sense. Other parameters are needed to describe the finer features of the spatial correlation structure (Ching and Phoon 2019).

In design, we frequently are more interested in the scale of fluctuation relative to the characteristic length of the structure (e.g., footing width, slope height, retaining wall height, or tunnel diameter). A scale of fluctuation that is much longer than the characteristic length of the structure is practically infinite, in the sense that the volume of soil that influences soil–structure interaction can be regarded as homogeneous. The notion of a worst-case scale of fluctuation discussed herein also is related to the ratio of the scale of fluctuation to the characteristic length of the geotechnical structure.

The concept of a scale of fluctuation, sometimes referred to as a spatial correlation length, originated in geostatistics for geology. This began with the variogram, which describes the amount of spatial dependence between two locations, as is explained in the next section.

An important application of the variogram is kriging. Kriging is an interpolation method originally developed by Krige (1951, 1966) for predicting ore grades in spatially varying gold mines. It interpolates known points and uses a weighted average of a function of the covariance between them to obtain the average value at an unknown location. It has a sound theoretical basis in the form of minimizing mean square error, not entirely different from

[1]Geotechnical Software Developer, Rocscience, Inc., 54 St. Patrick St., Toronto, ON, Canada M5T 1V1. Email: brigid.cami@rocscience.com

[2]Geomechanics Specialist, Rocscience, Inc., 54 St. Patrick St., Toronto, ON, Canada M5T 1V1. Email: sina.javankhoshdel@rocscience.com

[3]Professor, Dept. of Civil and Environmental Engineering, National Univ. of Singapore, Blk E1A, #07-03, 1 Engineering Dr., Singapore 117576 (corresponding author). ORCID: https://orcid.org/0000-0003-2577-8639. Email: kkphoon@nus.edu.sg

[4]Professor, Dept. of Civil Engineering, National Taiwan Univ., #1, Roosevelt Rd. Section 4, Taipei 10617, Taiwan. ORCID: https://orcid.org/0000-0001-6028-1674. Email: jyching@gmail.com

Note. This manuscript was published online on July 31, 2020. Discussion period open until December 31, 2020; separate discussions must be submitted for individual papers. This paper is part of the ***ASCE-ASME Journal of Risk and Uncertainty in Engineering Systems, Part A: Civil Engineering***, © ASCE, ISSN 2376-7642.

regression, except the measured points are correlated rather than independent (Brockwell and Davis 1991). This method became quickly popular in geostatistics and now is used in a wide array of disciplines.

The application of the random field to model spatial variability in geotechnical engineering was popularized by Vanmarcke (1977). Two concepts distinct from geostatistics became popular: (1) the scale of fluctuation that unifies autocorrelation function models and the implicit assumption that the scale of fluctuation is more important than the detailed mathematical form of the ACF (e.g., Markovian or Gaussian); and (2) spatial averaging and the variance reduction function (which also is related to the scale of fluctuation). Vanmarcke's (1983) key premise stated that all measurements involve spatial averaging, and therefore detailed differences in the spatially varying field are averaged out and the variance of the averaged field is smaller than that of the original field. This reduction is quantified by the variance reduction function. Recent literature demonstrated that spatial averaging in the Vanmarcke sense is not always the key mechanism in geotechnical engineering problems. An important mechanism not discussed by Vanmarcke (1977, 1983) is the worst-case scale of fluctuation, which is explained below.

A series of random finite-element papers, including those by Fenton and Griffiths (2003), Jaksa et al. (2005), Fenton et al. (2007), Breysse et al. (2007), Ching et al. (2017a), Luo et al. (2016), and Zhu et al. (2018), showed that a critical or worst-case scale of fluctuation exists for a variety of problems. Javankhoshdel et al. (2017) and Shahmalekpoor et al. (2020) reported the worst-case spatial correlation length using random limit equilibrium as well. The worst-case scale of fluctuation is defined as the scale of fluctuation value that results in the highest probability of failure. It also has been identified as the case producing the lowest mean response, such as the lowest bearing capacity of a shallow foundation installed in a spatially variable soil. If the response were to be equal to the spatial average along a prescribed slip surface in the Vanmarcke's (1977) sense, the mean response will be equal to the mean of the random field. This is a theoretical result arising from Vanmarcke's (1977) definition of the spatial average as a stochastic line, surface, or volume integral of a random field in a prescribed domain. In other words, the limits of the integral are constants. It does not depend on the scale of fluctuation, and certainly a worst-case will not appear under the notion of a spatial average as defined by Vanmarcke (1977, 1983). The worst-case scale of fluctuation, whenever it exists, is particularly useful for design when sufficient data are not available to estimate the scale of fluctuation directly. Ching et al. (2017a) compiled a table of worst-case scales of fluctuation reported in previous studies, which is reproduced in Table 1 with minor updates.

The concept of the worst-case scale of fluctuation has been explained in a series of papers using the concept of mobilized strength and modulus (Ching and Phoon 2013a, b, 2014; Hu and Ching 2015; Ching et al. 2016a, b, e, 2017b, c). The idea of converting a complex spatially heterogeneous medium to an equivalent (in some sense) homogeneous medium is comparable to the classical homogenization theory in micromechanics (Paiboon et al. 2013), except the equivalency principle is different. This concept is essentially a generalization of the classical spatial average, which was found to be limited to situations in which the failure path is constrained (e.g., side resistance of pile). It does not work for a failure path that is emergent (i.e., one that is the solution of a boundary value problem), such as a slope failure. It is evident that this path cannot be represented by a stochastic line integral with constant

Table 1. Worst-case scale of fluctuations reported in previous studies

Study	Problem type	Worst-case definition	Characteristic length	Worst-case scale of fluctuation
Jaksa et al. (2005)	Settlement of nine-pad footing system	Underdesign probability is maximal	Footing spacing (S)	$1 \times S$
Fenton and Griffiths (2003) Soubra et al. (2008)	Bearing capacity of a footing on c-ϕ soil	Mean bearing capacity is minimal	Footing width (B)	$1 \times B$
Fenton et al. (2005)	Active lateral force for retaining wall	Underdesign probability is maximal	Wall height (H)	$0.5–1 \times H$
Fenton and Griffiths (2005)	Differential settlement of footings	Underdesign probability is maximal	Footing spacing (S)	$1 \times S$
Breysse et al. (2005)	Settlement of footing system	Footing rotation is maximal Mean different settlement between footings is maximal	Footing spacing (S) Footing spacing (S) and footing width (B)	$0.5 \times S$ $f(S, B)$ (no simple equation)
Griffiths et al. (2006)	Bearing capacity of footing(s) on $\phi = 0$ soil	Mean bearing capacity is minimal	Footing width (B)	$0.5–2 \times B$
Vessia et al. (2009)	Bearing capacity of footing on c-ϕ soil	Mean bearing capacity is minimal (anisotropic 2D variability)	Footing width (B)	$0.3–0.5 \times B$
Ching and Phoon (2013a, b)	Overall strength of soil column	Mean strength is minimal	Column width (W)	$1 \times W$ (compression) $0 \times W$ (simple shear)
Ahmed and Soubra (2014)	Differential settlement of footings	Underdesign probability is maximal	Footing spacing (S)	$1 \times S$
Hu and Ching (2015)	Active lateral force for retaining wall	Mean active lateral force is maximal	Wall height (H)	$0.2 \times H$
Stuedlein and Bong (2017)	Differential settlement of footings	Underdesign probability is maximal	Footing spacing (S)	$1 \times S$
Ali et al. (2014)	Risk of infinite slope	Risk of rainfall induced slope failure is maximal	Slope height (H)	$1 \times H$
Pan et al. (2018)	Stress–strain behavior of cement-treated clay column	Peak global strength	Column diameter (D)	$2 \times D$

Source: Updated from Ching et al. (2017a).

integration limits. Hicks (2012), Hicks and Nuttall (2012), and Hicks et al. (2019) introduced a similar idea of an effective property that can be back-figured numerically from the response of a structure.

Ching and Phoon (2018) and Ching et al. (2019) further noted that the scale of fluctuation is a necessary but not a sufficient characterization of the ACF. They proposed a more complete characterization consisting of the scale of fluctuation and a smoothness parameter. This requires the adoption of a two-parameter autocorrelation function such as the powered exponential model and the Whittle–Matérn (WM) model. All classical autocorrelation functions, such as those in Table 2, are one-parameter models. This review paper focuses primarily on the scale of fluctuation, as few papers have characterized the smoothness parameter for real soil data.

Due to the importance of the scale of fluctuation, various methods have been developed to characterize this parameter from soil data, particularly cone penetration test (CPT) measurements, which are the most commonly used method of obtaining near-continuous field data. The scale of fluctuation can be estimated from CPT data using methods such as the method of moments (e.g., Tang 1979; Lacasse and Nadim 1996; Uzielli et al. 2005; Zhang and Dasaka 2010), maximum-likelihood estimation (MLE) (e.g., DeGroot and Baecher 1993; Fenton 1999; Hicks and Onisiphorou 2005; Jaksa et al. 2005; Lloret-Cabot et al. 2014), and Bayesian analysis (e.g., Wang et al. 2010; Cao and Wang 2012; Tian et al. 2016).

Estimating the scale of fluctuation in the most general setting in which all parameters are unknown, including the shape of the trend function and the autocorrelation function, and in the presence of limited data (e.g., one CPT sounding) may not be tractable. Ching et al. (2017a) called this the identifiability problem. The problem is more tractable in the presence of multiple CPT soundings (Ching et al. 2016d, e; Ching and Phoon 2017; Xiao et al. 2019).

The purpose of this paper is twofold. The paper first provides an overview of the methods available for estimating the scale of fluctuation from CPT data, along with two examples for comparing the methods. Second, it provides a database table of horizontal and vertical scale of fluctuation values in different locations and for different geomaterials. This tabulation is important because commercial software such as Slide2 version 2018 and SVSlope version 2009, which can analyze geotechnical problems with 2D spatial variability, and SLOPE/W version 2012, which can analyze geotechnical problems with one-dimensional (1D) spatial variability, increasingly are expanding the reach of their analyses from homogeneous (or layered) soils to more realistic spatially varying soils. For cases with insufficient field data where engineers find the scale of fluctuation difficult to estimate, this table can serve as an important reference to provide a sense of the probable range of values for sensitivity analyses.

Past random finite-element studies have demonstrated that the probability of failure is a function of the spatial correlation structure, which may include other characteristics of the autocorrelation model in addition to the scale of fluctuation such as the smoothness, nonmonotonicity, and degree of anisotropy (i.e., the ratio of vertical to horizontal scales of fluctuation). The sensitivity of the probability of failure or other quantities of interest to the designer [e.g., resistance factor in the load and resistance factor design (LRFD)] to the scale of fluctuation or other characteristics of the autocorrelation model has not been studied systematically. The relation between scales of fluctuation for different soil parameters currently is unknown. Cross-correlated vector fields involving multiple soil parameters currently are simulated assuming that all soil parameters follow a single autocorrelation model in the absence of data. These issues are important to random field applications, but they are outside the scope of this review paper, which focuses only on what have been characterized empirically from actual soil data in the literature.

Estimating Scale of Fluctuation from CPT Data

Spatial variability generally is characterized by traditional methods of time-series analysis used in statistics. This means that the value

Table 2. Common autocorrelation models and their frequency of usage in Table S1

Autocorrelation model	Correlation as a function of lag τ	ν	Frequency of usage (%)
Markovian (single exponential)	$\rho(\tau)=\exp\left\{\frac{-2\lvert\tau\rvert}{\theta}\right\}$	0.5	48
Second-order Markov	$\rho(\tau)=\left(1+4\frac{\lvert\tau\rvert}{\theta}\right)\exp\left\{-4\frac{\lvert\tau\rvert}{\theta}\right\}$	1.5	5
Third-order Markov	$\rho(\tau)=\left(1+\frac{16}{3}\frac{\lvert\tau\rvert}{\theta}+\frac{256}{27}\left(\frac{\lvert\tau\rvert}{\theta}\right)^2\right)\exp\left\{-\frac{16}{3}\frac{\lvert\tau\rvert}{\theta}\right\}$	2.5	New to geotechnical practice
Gaussian (squared exponential)	$\rho(\tau)=\exp\left\{-\pi\left(\frac{\lvert\tau\rvert}{\theta}\right)^2\right\}$	∞	19
Spherical	$\rho(\tau)=\begin{cases}\frac{4}{3}-2\left\lvert\frac{\tau}{\theta}\right\rvert+\frac{2}{3}\left\lvert\frac{\tau}{\theta}\right\rvert^3, & \text{if } \lvert\tau\rvert\le\theta;\\ 0, & \text{otherwise}\end{cases}$	—	7
Cosine exponential	$\rho(\tau)=\exp\left\{-\frac{\lvert\tau\rvert}{\theta}\right\}\cos\left\{\frac{\lvert\tau\rvert}{\theta}\right\}$	—	8
Binary noise	$\rho(\tau)=\begin{cases}1-\lvert\tau\rvert/\theta, & \text{if } \lvert\tau\rvert\le\theta\\ 0, & \text{otherwise}\end{cases}$	—	12
Whittle–Matérn	$\rho(\tau)=\frac{2}{\Gamma(\nu)}\left\{\frac{\sqrt{\pi}\Gamma(\nu+0.5)\lvert\tau\rvert}{\Gamma(\nu)\theta}\right\}^{\nu}K_{\nu}\left\{\frac{\sqrt{\pi}\Gamma(\nu+0.5)\lvert\tau\rvert}{\Gamma(\nu)\theta}\right\}$	—	—

Note: θ = scale of fluctuation; ν = smoothness parameter that reduces Whittle–Matérn model to specific one-parameter autocorrelation model (e.g., $\nu=0.5$ produces Markovian exponential model); model name third-order Markov is coined in this paper; Γ = gamma function (Abramowitz and Stegun 1970); and K_v = modified Bessel function of second kind with order ν (Abramowitz and Stegun 1970); Appendix derives equation for Whittle–Matérn model such that it integrates to θ as in Eq. (2).

of a parameter at a given location generally is described by the sum of a trend and a zero-mean spatial variability [Eq. (1)]. As with measurements in time, soil property measurements that are closer together in space are more similar in value. For simplicity, the methods outlined below apply to the measurements from a single CPT sounding, from which the vertical scale of fluctuation needs to be estimated. The methods easily can be extended to 2D or 3D if the ACF is assumed to be separable. To the authors' knowledge, this separability assumption has not been validated by real data.

$$X_i = X(s_i) = T(s_i) + \epsilon(s_i), \quad i = 1, \ldots, k \tag{1}$$

In Eq. (1) above, $X(s_i)$ or X_i = value of soil property at location s_i, where s_i = vertical depth below ground surface, for example; k = total number of measurements; $T(s_i)$ = trend component; and $\epsilon(s_i)$ = spatial variability component. The scale of fluctuation describes the distance over which the spatial variability components $\epsilon(s_i)$ are correlated among themselves. All methods described subsequently assume that the mean and variance of the data already have been estimated using common methods. The current state of the art is capable of estimating all random field parameters, such as the mean, variance, and scale of fluctuation, simultaneously (e.g., Ching and Phoon 2017; Ching et al. 2017a). Efficient estimation of random field parameters and simulation of conditional random fields in a 3D setting is now possible (Ching et al. 2020).

The separation between T and ϵ is the famous detrending problem. Characterizing ϵ as a stationary random field without making any assumptions (i.e., determining all random field parameters simultaneously without any assumptions) is a difficult problem, particularly for one CPT sounding (Ching et al. 2016c, d, 2017a; Ching and Phoon 2017). Ching et al. (2016d) demonstrated that this difficulty manifests itself as statistical uncertainties in the context of Bayesian estimation, which in turn results in less precise probabilities of failure for limit states involving random fields. This unfavorable impact on reliability-based design is of practical importance. Jiang and Huang (2018) proposed a nonstationary random field model which can account for the uncertainties of the trend component T. The detrending problem can be avoided by characterizing X_i as a nonstationary random field, but this also is a difficult problem in the absence of data. Geostatistics now is using the multiple point method (Mariethoz and Caers 2014); however, this method requires image data beyond CPT. Another promising approach is based on Bayesian compression sampling (BCS) (Wang and Zhao 2016, 2017). Wang et al. (2017) subsequently combined BCS with the Karhunen–Loève (KL) expansion (called a BCS-KL random field generator) to simulate realizations (or sample paths) directly from sparse measurements (Wang et al. 2019a). The sample path is needed because the failure mechanism at the ultimate limit state usually is restricted to slip curves, rather than mobilizing the entire soil mass. The BCS-KL generator is nonparametric and data-driven. No predetermined function forms are needed for the marginal probability density function or covariance function of the random field. Therefore, the BCS-KL generator is readily applicable to non-Gaussian and nonstationary random fields, including those with nonstationary autocovariance structures (Montoya-Noguera et al. 2019) and those with unknown trend functions without detrending (Wang et al. 2019b). In addition, the BCS-KL generator may be extended readily to simulate cross-correlated bivariate random fields (Zhao and Wang 2018). An important open question is whether the basis functions in BCS (which are prescribed) can reproduce correctly the finer details of some sample paths such as those produced by the Whittle–Matérn ACF when there are sufficient measurements (convergence) (Phoon and Wang 2019). A second related question is whether it can retain its key practical advantage of representing such rough sample paths using sparse measurements (rate of convergence) (Phoon and Wang 2019).

Different Measures of Spatial Correlation

In this paper, the scale of fluctuation (θ) is defined as the area under the autocorrelation function, $\rho(\tau)$ (Vanmarcke 1983)

$$\theta = \int_{-\infty}^{\infty} \rho(\tau) d\tau = 2\int_{0}^{\infty} \rho(\tau) d\tau \tag{2}$$

What is referred to as scale of fluctuation, correlation length, or autocorrelation distance can result from several different definitions, all of which may be used loosely with less precision than desired in the geotechnical literature. For example, the factor of 2 in Eq. (2) often is omitted, resulting in both θ and $\theta/2$ being referred to as the scale of fluctuation. The scale of fluctuation also may be mistaken as the model parameter, rather than the θ defined in Eq. (2). For example, one definition of the single exponential autocorrelation model is $\rho(\tau) = \exp\{(-|\tau|)/a\}$, where a is the model parameter. However, in Table 2 it is defined as $\rho(\tau) = \exp\{(-2|\tau|)/\theta\}$. The version in Table 2 is the harmonized version to ensure $2\int_0^\infty \exp\{(-2|\tau|)/\theta\} = \theta$ (Vanmarcke 1983). Using the model parameter version, however, gives $2\int_0^\infty \exp\{(-|\tau|)/a\} = 2a$, meaning that $\theta = 2a$. This is the difference between solving for the model parameter, a, and the scale of fluctuation, θ. The confusion results from the model parameter being taken to be the scale of fluctuation. For the squared exponential autocorrelation model, the integral of the model parameter version, $\rho(\tau) = \exp\{-(|\tau|/a)^2\}$, is $\sqrt{\pi}a$, whereas the version in Table 2 has been harmonized to integrate to θ, meaning that $\theta = \sqrt{\pi}a$. If a study were to take a to be the scale of fluctuation, in reality it would be different from the scale of fluctuation by a factor of $1/\sqrt{\pi}$.

In this study, the scale of fluctuation refers to θ as defined in Eq. (2), and all the autocorrelation models are taken to be those in Table 2, which have been harmonized to integrate to θ.

Estimation Methods

A simple way to visualize the physical meaning of scale of fluctuation is through the rule of thumb estimation method in Fig. 1 (Spry et al. 1988). This method averages out the distances between CPT intersections (called zero crossings in the signal

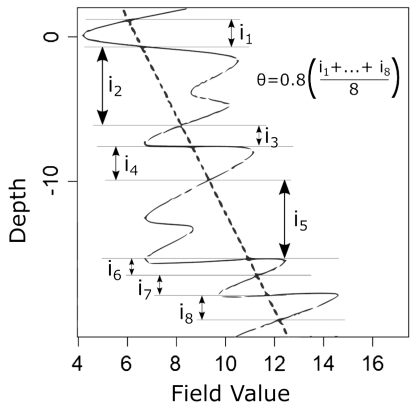

Fig. 1. Illustration of the rule of thumb method for estimating the scale of fluctuation.

processing literature) with the trendline. The scale of fluctuation can then be estimated as 80% of this average distance.

The rule of thumb method was derived under the assumption of a Gaussian random field governed by the squared exponential autocorrelation function based on signal processing theory (e.g., Rice 1944; Zhu et al. 2019). The method provides a reasonable estimate when the assumptions (i.e., Gaussian marginal distribution and squared exponential autocorrelation function) are valid and the length of the measurement profile is sufficiently long. Otherwise, it could produce biased estimates of the scale of fluctuation. It undoubtedly is attractive to practitioners because the method is straightforward, but the authors recommend using it only for smooth sample paths that plausibly may arise from the squared exponential autocorrelation function.

For wide applicability, the most common methods used to estimate the scale of fluctuation can be grouped into three categories: (1) the method of moments, (2) maximum-likelihood estimation, and (3) Bayesian analysis. The first two categories are frequentist methods, with the method of moments being the most commonly used method.

To best understand the differences between the various estimation methods, the scale of fluctuation from a real CPT sounding was evaluated numerically using the frequentist methods. This also was done for an ideal simulated example in which the correct scale of fluctuation was known.

Method of Moments

The method of moments is a standard method of estimating population parameters in statistics. With the method of moments, the sample or empirical moments are set equal to the theoretical moments, and the parameters of interest are solved so as to minimize the error between the two.

The method of moments can be further subdivided into two categories: (1) autocorrelation or autocovariance function fitting, and (2) semivariogram or variogram fitting.

The power spectral density (PSD) function is the Fourier transform of the autocorrelation function. The PSD is more commonly encountered in random vibration problems. To the authors' knowledge, it is less common to estimate PSD than the autocorrelation, although there are some interesting attempts in this direction (Phoon and Fenton 2004).

Autocorrelation or Autocovariance Function Fitting

The scale of fluctuation is estimated by fitting empirical autocorrelation or autocovariance values typically computed at discrete lags to the theoretical models in Table 2 (e.g., Vanmarcke 1977; DeGroot and Baecher 1993; Fenton 1999; Baecher and Christian 2003; Wackernagel 2003; Uzielli et al. 2005; Lloret-Cabot et al. 2014). With this method, the theoretical autocorrelation model is set equal to the sample autocorrelation function, and the scale of fluctuation is determined using a fitting method such as least squares. This similarly can be done with the autocovariance function, which is the product of the autocorrelation model and the variance of the data.

The autocorrelation model describes the correlation between the same soil parameter measured at different locations. The cross-correlation describes the correlation between different soil parameters measured at the same location. Cross-correlation is not covered in this paper because it has been detailed elsewhere (Ching et al. 2016c). Several commonly used autocorrelation models are summarized in Table 2, in which $\rho(\tau)$ represents the correlation coefficient at a given lag distance τ between two points. The lag describes a multiple of the measurement interval. For illustration, if the measurement interval in a CPT sounding is 0.1 m, $\rho(\tau_1)$ describes the correlation coefficient between two points that are 0.1 m apart; $\rho(\tau_2)$ describes the correlation between two points that are 0.2 m apart, and so on. Some of the classical autocorrelation models are special cases of the more general two-parameter Whittle–Matérn model (Ching et al. 2019). The autocorrelation function can be obtained by substituting an appropriate smoothness parameter ν into the Whittle–Matérn model (Table 2). There effectively are only four such special cases, based on special values of $\nu = p + 0.5$, where $p = 0, 1, 2, 3$. The case of $p = 0$ produces the Markovian model. The case of $p = 1$ produces the second-order Markovian model. To the best of the authors' knowledge, the case of $p = 2$ is entirely new to geotechnical practice. Because this new autocorrelation model constitutes the product of an exponential function and a quadratic function, it is named a third-order Markovian model in this paper. The cases of $p = 3$ and higher are practically indistinguishable from the Gaussian model ($\nu = \infty$) (Rasmussen and Williams 2006). The frequency of usage column denotes the percentage of studies in Table S1 that adopted a particular model. The Markovian autocorrelation model is by far the most popular, accounting for almost half of studies surveyed in this review.

The experimental autocorrelation function is

$$\hat{\rho}(\tau_j) = \frac{1}{\hat{\sigma}^2 k}\sum_{i=1}^{k-j}(X_i - \hat{\mu})(X_{i+j} - \hat{\mu}), \quad j = 0, \ldots, k-1 \tag{3}$$

where $\hat{\rho}(\tau_j)$ = experimental correlation coefficient between two points separated by τ_j; $\hat{\sigma}^2$ = sample variance of data; $\hat{\mu}$ = sample mean of data; k = total number of measurement points; and i = total number of pairs of points separated by lag τ_j.

An important note is warranted here. The geotechnical literature often cites Eq. (3) with $(k - j)$ in the denominator instead of k. Although this is a natural estimator of the autocorrelation at lag τ_j, it results in a correlation matrix with a negative eigenvalue, which violates a key requirement of correlation matrices: that they must be positive definite (Priestley 1981; Fenton 1999). This requirement is important because allowing a negative eigenvalue is akin to allowing a negative variance, which is not possible. Although the revised version [Eq. (3)] is valid, it is not well emphasized that it is not robust (Chang and Politis 2016). This is explored further in section "Example 3: Experimental Autocorrelation Equation."

The error between the theoretical and experimental functions can be minimized to find scale of fluctuation (θ) using various methods, the most common of which is least squares. Using least squares, Eq. (3) is minimized with respect to θ by taking the derivative, setting it equal to zero, and solving for θ

$$\text{Error} = \sum_{j=1}^{k}[\hat{\rho}(\tau_j) - \rho(\tau_j)]^2 \tag{4}$$

The practical difficulty with this method is that the statistical uncertainty associated with the correlation between two points increases with lag distance. This is because the number of pairs of sampled points decreases with lag distance. For example, if the length of the CPT sounding is L, then there is only one pair of points with a lag distance of L. Eq. (4) assumes that all estimates from Eq. (3) are equally accurate. A weighted regression with less weight assigned to correlations at larger lags to account for larger statistical uncertainties is more logical. Alternately, Eq. (4) is applied only to lag distances at which the correlations can be more reliably estimated. The rule of thumb is to keep lag distance shorter than $L/4$ (Lumb 1975) or to use correlation coefficients exceeding

Bartlett's limits (Uzielli et al. 2005). Priestley (1981) provided an excellent compilation of known theoretical results pertaining to the biasness, variances, and covariances of the sample autocorrelation function at different lags. Many of these results were reported in the classical paper by Bartlett (1946). Nevertheless, Priestley (1981) noted that the sampling properties of the sample autocorrelation function are extremely complicated and only approximate asymptotic results may be obtained.

Finally, Lloret-Cabot et al. (2014) introduced an autocorrelation function fitting method that uses a conditional random field to calculate the scale of fluctuation. This works by creating a random field from the initial estimates of the scale of fluctuation, and then re-estimating the scale of fluctuation from the conditional random field. The conditional random field is the random field created using the CPT data and the initial scale of fluctuation estimates. The process is repeated for a number of iterations.

Semivariogram or Variogram Fitting

A semivariogram is a plot of $\gamma(\tau)$ on the y-axis and of lag distance on the x-axis, the theoretical equation of which follows:

$$\gamma(\tau) = \frac{1}{2}\text{var}(X(s_i) - X(s_i + \tau)) \tag{5}$$

This is related to the autocovariance function by $\gamma(\tau) = \text{sill} - \text{cov}(\tau)$, where sill is the height that the semivariogram reaches when it levels off. A typical semivariogram is shown in Fig. 2. The range is the corresponding x-coordinate of the sill, or the smallest distance over which two points are no longer correlated [$\text{cov}(\tau) = 0$], and hence $\gamma(\tau) = \text{sill}$. The range often is taken to mean the scale of fluctuation. Although both parameters quantify a similar concept (the distance over which points are correlated), they are not always the same. The range here is a model parameter, and not the scale of fluctuation as defined in Eq. (2). The nugget in Fig. 2 is the quantity at zero lag and is interpreted as measurement noise in geotechnical engineering (Baecher 1986; ArcGis Desktop Help 2019).

Although there is a lot of work with the semivariogram in other disciplines such as geology, soil sciences, geophysics, ground water, and reservoir management, among others (Matheron 1963; McCuen et al. 1988; White and Ayyub 1990; Cressie 1992; Chiles and Delfiner 2009), this review is restricted to geotechnical engineering, in which the depth of interest covers only the typical depths of underground structures (Anderson et al. 2008).

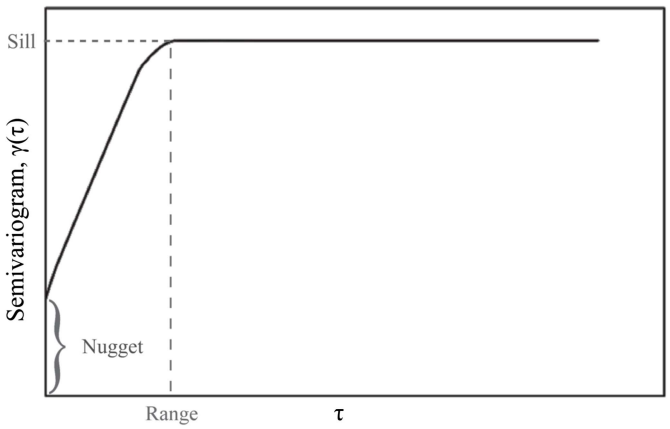

Fig. 2. Definition of sill, nugget, and range in a typical semivariogram.

The experimental semivariogram follows:

$$\hat{\gamma}(\tau) = \frac{1}{2k}\sum_{i=1}^{k}[X(s_i) - X(s_i + \tau)]^2 \tag{6}$$

The experimental semivariogram then is fitted to the theoretical semivariogram using a fitting method such as least squares to minimize the error between the two. A variogram, on the other hand, is defined simply as $2\gamma(\tau)$, and the same semivariogram procedure described previously is followed.

Maximum-Likelihood Estimation

Maximum-likelihood estimation is another commonly used method for estimating population parameters in statistics (DeGroot and Baecher 1993; Liu and Leung 2017; Liu et al. 2016). A limitation of this method is that a distribution must be assumed for the random field, such as normal and lognormal. As noted previously, the spatial variability component from Eq. (1) is described by an autocovariance or autocorrelation function.

The likelihood is defined as the likelihood of obtaining a certain distribution parameter, given the known CPT measurements. It is the product of the probabilities for each measurement, assuming that the measurements are independent. Because clearly this is not the case with spatial measurements, the data are put into matrix notation, where $\mathbf{V}$ represents the variance-covariance matrix. The off-diagonal components of $\mathbf{V}$ contain the covariance values between multiples of lags. These values are divided by the variance to obtain correlation coefficients, which then are set equal to one of the autocorrelation models in Table 2 to solve for θ.

Generally, the log-likelihood is easier to maximize than the likelihood. The log-likelihood equation, assuming a normal distribution is

$$L(\boldsymbol{\phi}|\boldsymbol{Y}) = -\frac{n}{2}\ln(2\pi) - \frac{1}{2}\ln(|\boldsymbol{V}|) - \frac{1}{2}(\boldsymbol{Y} - \boldsymbol{X\beta})^{\mathrm{T}}\boldsymbol{V}^{-1}(\boldsymbol{Y} - \boldsymbol{X\beta}) \tag{7}$$

where $\boldsymbol{\phi}$ = vector of unknown parameters which are not yet determined; $\boldsymbol{Y}$ = vector of CPT measurements; $\boldsymbol{X\beta}$ = sample mean of $\boldsymbol{Y}$; $\mathbf{V}$ = variance-covariance matrix; and $|\mathbf{V}|$ = determinant of $\mathbf{V}$.

Eq. (7) assumes that the data have a normal distribution. If the distribution of the data appears to be significantly different from the normal, then the likelihood should be calculated with the corresponding density function based on some goodness-of-fit criterion. The examples in the next section use Eq. (7) and the maximization algorithm outlined by Xiao et al. (2018).

This method was used by Xiao et al. (2019) in a three-dimensional setting. Although the computation of $\mathbf{V}^{-1}$ potentially is costly, Xiao et al. (2019) proposed an efficient scheme for obtaining it under the assumption that the autocorrelation is separable in the vertical and horizontal directions. Ching et al. (2020) fills a gap in efficient conditional simulation of three-dimensional fields that was left unresolved by Xiao et al. (2019). Ching et al. (2019) noted that all classical autocorrelation models in Table 2 are one-parameter models that can fit only the scale of fluctuation. These models cannot fit the smoothness parameter, which is distinct from the scale of fluctuation, and can give misleading estimation results for the scale of fluctuation when implemented with MLE. Ching et al. (2019) recommended the use of a two-parameter Whittle–Matérn model to estimate the scale of fluctuation and smoothness parameter at the same time. The maximum-likelihood method was found to be necessary in this estimation process.

Bayesian Analysis

The methods described previously follow frequentist analysis methods. This means that only the known data (values measured at each CPT increment) are used to calculate the scale of fluctuation. Frequentist methods assume that the scale of fluctuation is an unknown constant which can be solved for using one of the aforementioned methods.

Bayesian analysis assumes that the unknown probabilistic model parameters such as the mean, coefficient of variation, and scale of fluctuation are not constants, but rather random variables (possibly correlated). As such, using Bayesian analysis, the scale of fluctuation distribution must be solved for. This is done by first defining a prior distribution for the scale of fluctuation, which, if sufficient data are not present, can be set to a relatively uninformative distribution, such as a uniform distribution between the minimum and maximum values of the scale of fluctuation typically found for a given geomaterial. The section "Literature Review of Typical Scales of Fluctuation" provides additional guidance on typical minimum and maximum values. The posterior, or updated distribution then is determined from Bayes' rule

$$p(\boldsymbol{\phi}|\boldsymbol{Y}) = \frac{p(\boldsymbol{Y}|\boldsymbol{\phi})p(\boldsymbol{\phi})}{p(\boldsymbol{Y})} \propto p(\boldsymbol{Y}|\boldsymbol{\phi})p(\boldsymbol{\phi}) \tag{8}$$

where $\boldsymbol{\phi}$ = vector of unknown probabilistic model parameters which are not yet determined; $\boldsymbol{Y}$ = vector of CPT measurements; $p(\boldsymbol{\phi})$ = prior distribution; $p(\boldsymbol{\phi}|\boldsymbol{Y})$ = posterior distribution; and p = probability distribution. The vertical bar represents the conditional probability of the first term given the second. Therefore, the result of Eq. (8), $p(\boldsymbol{\phi}|\boldsymbol{Y})$, is a set of scale of fluctuation values and their corresponding probabilities, or a distribution. The most probable scale of fluctuation value is a reasonable choice if only one value is needed for random field simulation.

Application of Bayesian analysis has been attempted within very general and very difficult settings, in which the shape of the trend function is unknown and only one CPT sounding is available (Ching et al. 2015, 2016d, 2017a; Ching and Phoon 2017; Ching et al. 2020). This Bayesian approach is very powerful and now is extended further to a broader MUSIC-X context (MUSIC = Multivariate, Uncertain and unique, Sparse, Incomplete, and potentially Corrupted data and X = spatially variable data). MUSIC-X encapsulates all possible site investigation data in the most realistic setting to date (Ching and Phoon 2019). One clear advantage of the Bayesian approach is that statistical uncertainty is included automatically, because the probabilistic model parameters are considered as random. The frequentist approach requires a separate analysis based on sampling theory to characterize statistical uncertainty. This advantage is critical for geotechnical engineering, because sample sizes are small in many cases (Phoon 2017) and one can argue that the current prevalent practice of reporting statistics such as the mean, coefficient of variation, and scale of fluctuation as numbers without the associated statistical uncertainty (which can be significant) is not suitable for geotechnical engineering. The preferred practice is to present the mean, coefficient of variation, scale of fluctuation, and other parameters as a 95% confidence interval. This was not carried out in the this paper because the source data to perform Bayesian analysis typically are not reported in many papers.

Examples

To best understand the differences in the scale of fluctuation that can result from the frequentist estimation methods, two examples are provided. The first used a CPT sounding from a study, the scale of fluctuation of which was estimated previously using a method of moments. The second is a simulated example in which the scale of fluctuation is known.

These examples then were used to estimate the scale of fluctuation using (1) rule of thumb, (2) autocorrelation function fitting with two different autocorrelation models, and (3) maximum-likelihood estimation with two different autocorrelation models.

An additional example is presented to demonstrate the problem with the experimental autocorrelation function that often is cited in the geotechnical literature.

Example 1: Świebodzice CPT Sounding

This example uses a CPT sounding from Świebodzice, Poland (Bagińska et al. 2012), the scale of fluctuation of which was estimated by Pieczyńska-Kozłowska (2015). The cone tip resistance q_c for this Świebodzice CPT sounding is shown in Fig. 3.

Pieczyńska-Kozłowska (2015) used various autocorrelation models and detrending methods and compared the resulting scale of fluctuations, which were estimated using the methods of moments. For comparison purposes, the CPT was only linearly detrended and is used subsequently. The results from Pieczyńska-Kozłowska (2015) are summarized in Table 3.

The detrended CPT data then were used to estimate the scale of fluctuation using the (1) rule of thumb, (2) autocorrelation function fitting with two types of autocorrelation models, and (3) maximum-likelihood estimation with two types of autocorrelation models. The results are summarized in Table 4. Although the rule of thumb, method of moments, and Gaussian MLE were in agreement with the results from Pieczyńska-Kozłowska (2015) and with each other, the Markovian MLE estimate is larger than the others. This was due

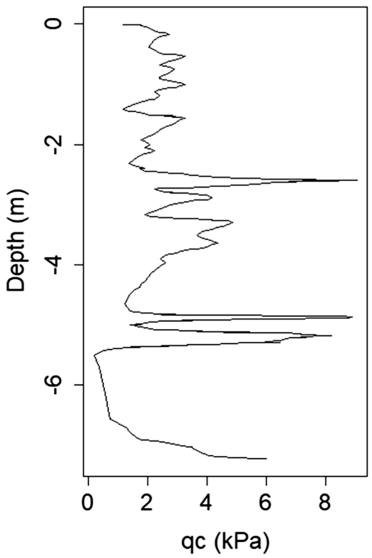

Fig. 3. Świebodzice CPT for q_c.

Table 3. Pieczyńska-Kozłowska (2015) linearly detrended scale of fluctuation results (meters)

Method	Markov autocorrelation	Gaussian autocorrelation
Vanmarcke method (autocorrelation function fitting)	0.28	0.22
Rice method (rule of thumb method based on mean crossing distance)	0.23	0.29

Table 4. Scale of fluctuation for q_c from Świebodzice CPT soundings, obtained using three different estimation methods (meters)

Estimation method	Scale of fluctuation
Rule of thumb	0.30
Method of moments fitting	
Markovian model	0.29
Gaussian model	0.26
Maximum-likelihood estimation[a]	
Markovian model (theoretical $\nu = 0.5$)	0.52
Second-order Markov model (theoretical $\nu = 1.5$)	0.40
Third-order Markov model (theoretical $\nu = 2.5$)	0.37
Gaussian model (theoretical $\nu = \infty$)	0.32
Whittle–Matérn model (theoretical ν unknown)	0.39 ($\nu = 1.69$)

[a]MLE requires inversion of correlation matrix. CPT measurements that are very closely spaced often result in a singular correlation matrix. Hence, MLE estimates were computed with CPT spacing of 0.15 m, whereas rule of thumb and method of moments estimates were computed with 0.05-m CPT spacing.

to the use of the Markovian autocorrelation with MLE. MLE is very sensitive to the origin of the classical one-parameter autocorrelation model, and hence it is less forgiving of a wrong choice for the autocorrelation model (Ching et al. 2019). For comparison, the scale of fluctuation and the smoothness parameter (ν) of the more general Whittle–Matérn model were estimated using MLE (Table 4). The ν value of 1.69 indicates that the second-order Markovian model may be a stronger contender ($\nu = 1.5$). Nonetheless, although the Whittle–Matérn model has a better chance of fitting empirical ACFs given the availability of two fitting parameters, there is no guarantee that it is the correct fit. Therefore, more robust estimation methods are needed. Although the autocorrelation model may be less important than the scale of fluctuation in the estimation of the variance reduction function (Vanmarcke 1983), it is incorrect to conclude that this is true for other quantities, such as the estimation of the scale of fluctuation itself. Ching and Phoon (2018) presented another example involving the estimation of a probability of failure for a failure mechanism not dominated by spatial averaging. The autocorrelation model is important in this context as well.

Example 2: Simulated Data

This example used data which were simulated to have an isotropic scale of fluctuation of 1 m. This means that the vertical scale of fluctuation was equal to the horizontal scale of fluctuation, and they both were 1 m. This was done using covariance matrix decomposition with the Cholesky method, as outlined by Li et al. (2019). The simulated field followed a normal distribution with a mean of 10 and a standard deviation of 2. The Markovian and Gaussian autocorrelation models were used to generate the fields. A Markovian random field with mesh size of 0.2 m in a 50-m-wide and 50-m-high space is shown in Fig. 4. The adopted random field parameters are reasonable (Phoon and Kulhawy 1999). Five equispaced vertical samples were taken from the field at $x = 5.0$, 15.0, 25.0, 35.0, and 45.0 m (Fig. 4). The sample at 45.0 m is shown in Fig. 5 as an example.

The scale of fluctuation was estimated using the same methods described in the previous example and averaged over 20 simulations. Because these data were simulated with a constant mean of 10, detrending was not necessary. The results are summarized in Tables 5 and 6.

This simulated example is important as a case in which the true scale of fluctuation is known, and the various methods can be evaluated based on how closely they approach this true value. It is immediately evident that the choice of autocorrelation model used

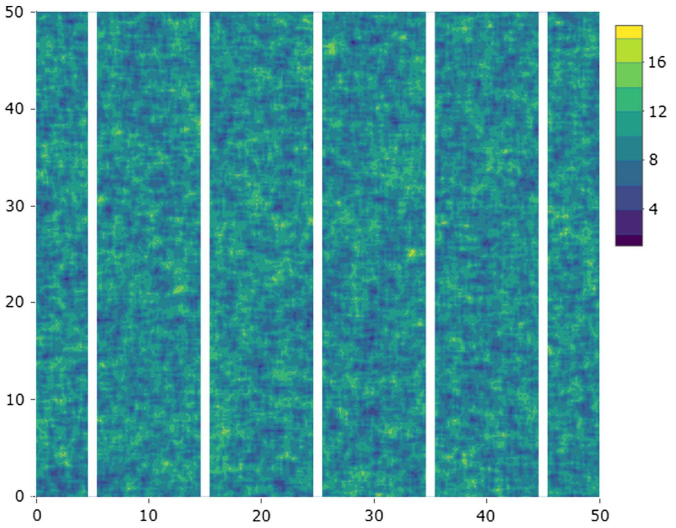

Fig. 4. Normal random field generated with a mean = 10, standard deviation = 2, and Markovian autocorrelation model with an isotropic scale of fluctuation of 1 m (vertical length = horizontal length = 1 m). The vertical sample locations are indicated with white lines.

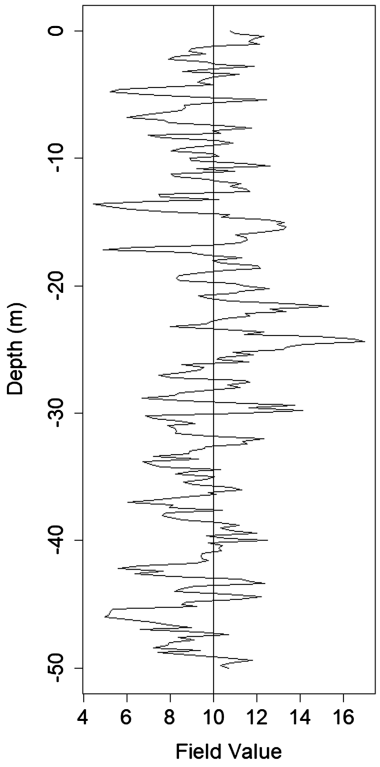

Fig. 5. Vertical sample taken at $x = 45.0$ m from the simulated field in Fig. 4. The mean of 10 is shown with a vertical line.

in the estimation has an impact on the estimate; this is especially prominent when using MLE. When the field is generated using the Markovian autocorrelation model (Table 5), the Markovian autocorrelation estimates give better results than the Gaussian model in both the method of moments and MLE cases. The MLE Gaussian result is very different from the Markovian result; this is due to MLE's sensitivity to the origin of the autocorrelation model, as discussed previously (Ching et al. 2019). This is confirmed in Table 6 for a Gaussian field generated with the same parameters;

Table 5. Scales of fluctuation estimated using methods of moments and MLE for data simulated with Markovian autocorrelation model (meters)

Estimation method	Average scale of fluctuation	Measurement location				
		5	15	25	35	45
Rule of thumb	**0.60**	0.60	0.63	0.58	0.58	0.59
Method of moments fitting						
Markovian autocorrelation model	**0.98**	1.07	0.98	0.94	0.90	1.00
Gaussian autocorrelation model	**0.89**	0.94	0.89	0.84	0.82	0.94
Maximum-likelihood estimation						
Markovian model (theoretical $\nu = 0.5$)	**0.97**	0.97	1.00	0.93	0.95	1.00
Second-order Markov model (theoretical $\nu = 1.5$)	**0.58**	0.58	0.59	0.60	0.57	0.58
Third-order Markov model (theoretical $\nu = 2.5$)	**0.51**	0.51	0.52	0.52	0.50	0.51
Gaussian model (theoretical $\nu = \infty$)	**0.42**	0.42	0.42	0.41	0.42	0.42
Whittle–Matérn model (theoretical ν unknown)	**1.04 ($\nu = 0.51$)**	0.99 (0.52)	1.05 (0.52)	1.13 (0.49)	1.06 (0.48)	0.97 (0.52)

Note: Average values indicated in bold. Values averaged over 100 values from 20 simulations sampled over 5 vertical profiles (Fig. 4).

Table 6. Scales of fluctuation estimated using methods of moments and MLE for data simulated with the Gaussian autocorrelation model (meters)

Estimation method	Average scale of fluctuation	Measurement location				
		5	15	25	35	45
Rule of thumb	**1.03**	1.04	1.00	0.99	1.07	1.06
Method of moments fitting						
Markovian autocorrelation model	**1.06**	1.11	1.10	0.98	1.03	1.06
Gaussian autocorrelation model	**1.01**	1.04	1.03	0.97	0.98	1.03
Maximum-likelihood estimation						
Markovian model (theoretical $\nu = 0.5$)	**3.11**	3.13	3.18	2.97	3.02	3.25
Second-order Markov model (theoretical $\nu = 1.5$)	**2.36**	2.35	2.37	2.36	2.33	2.37
Third-order Markov model (theoretical $\nu = 2.5$)	**1.97**	1.96	1.95	1.99	1.97	1.98
Gaussian model (theoretical $\nu = \infty$)	**0.94**	0.94	0.95	0.94	0.94	0.96
Whittle–Matérn model (theoretical ν unknown)	**1.02 ($\nu = 72.4$)**	1.02 (66.3)	1.00 (75.7)	1.04 (80.7)	1.02 (67.2)	1.02 (72.2)

Note: Average values indicated in bold. Values averaged over 100 values from 20 simulations sampled over 5 vertical profiles (Fig. 4).

the Markovian MLE estimate was much worse than the Gaussian MLE estimate. The differentiability at the origin of the autocorrelation model is related to the smoothness of a profile such as that shown in Fig. 5. This smoothness is distinct from the scale of fluctuation. Using MLE correctly requires selecting an appropriate classical one-parameter autocorrelation model that is consistent with smoothness of the observed profile. This caveat is not well recognized in the literature and in practice. Ching et al. (2019) recommended a more robust approach involving applying MLE in conjunction with a two-parameter Whittle–Matérn model that is flexible enough to capture the smoothness and the scale of fluctuation of the observed profile simultaneously. The results are given in the last rows of Tables 5 and 6. Because the Markovian and Gaussian models are special cases of the Whittle–Matérn model, the MLE is able to identify both the correct model and the correct scale of fluctuation in both tables. The ν values in Table 6 can be regarded as very large, which are consistent with the theoretical $\nu = \infty$ for the Gaussian model. Rasmussen and Williams (2006) pointed out that it is very difficult to distinguish between values of $\nu > 3.5$ from actual finite noisy data, and suggested that these ν values are sufficiently large as to be practically indistinguishable from $\nu = \infty$ for the Gaussian model.

Another interesting observation is that the rule of thumb or Rice method is very accurate when the field is generated with the Gaussian autocorrelation model. As previously mentioned, this is because this method was derived as a means of estimating a field that follows a Gaussian autocorrelation model.

Considering the fields generated with the Markovian autocorrelation model only, the histograms in Fig. 6 show the scale of fluctuation values estimated at each of the 5 locations, over the 20 simulations (100 values total), using Markovian method of moments and Markovian MLE. Using the method of moments leads to a wider range of estimated values with a less distinct mean value compared with MLE. This implies that with a small number of samples (as might be found in a real case study) the MLE would provide more accurate results. However, as has been noted, the MLE is highly sensitive to the assumed classical one-parameter autocorrelation model, whereas the method of moments is not. The conventional wisdom that the scale of fluctuation is sufficient for spatial variability analysis is perhaps slightly optimistic when one considers the preceding characterization problem.

Example 3: Experimental Autocorrelation Equation

It was explained previously that the geotechnical literature often cites the experimental autocorrelation equation [Eq. (3)] with $(k - j)$ in the denominator instead of k

$$\hat{\rho}(\tau_j) = \frac{1}{\hat{\sigma}^2(k-j)} \sum_{i=1}^{k-j} (X_i - \hat{\mu})(X_{i+j} - \hat{\mu}), \quad j = 0, \ldots, k-1 \tag{9}$$

However, this equation results in a correlation matrix with a negative eigenvalue, which violates the positive definiteness of correlation matrices. This is explored in this example as follows: a CPT sounding is simulated with five values; the first value is assumed to be measured at ground level, and the others are subsequent measurements into the ground at equal increments, δ. The five points were sampled from a normal distribution with a mean of 10 and variance of 4 (Table 7). The values are assumed to be detrended.

The variance of the data is calculated as $\hat{\sigma}^2 = 2.96$, and the mean is calculated as $\hat{\mu} = 10.26$ using standard methods. A normalized variable was defined as $\hat{X}_i = (X_i - \hat{\mu})/\hat{\sigma}$. The corresponding autocorrelation matrix then can be established for each τ_j

$$\begin{bmatrix} \frac{1}{5}\sum_{i=1}^{5}(\hat{X}_i)(\hat{X}_i) & \frac{1}{4}\sum_{i=1}^{4}(\hat{X}_i)(\hat{X}_{i+1}) & \frac{1}{3}\sum_{i=1}^{3}(\hat{X}_i)(\hat{X}_{i+2}) & \frac{1}{2}\sum_{i=1}^{2}(\hat{X}_i)(\hat{X}_{i+3}) & \frac{1}{1}\sum_{i=1}^{1}(\hat{X}_i)(\hat{X}_{i+4}) \\ \frac{1}{4}\sum_{i=1}^{4}(\hat{X}_i)(\hat{X}_{i+1}) & \frac{1}{5}\sum_{i=1}^{5}(\hat{X}_i)(\hat{X}_i) & \frac{1}{4}\sum_{i=1}^{4}(\hat{X}_i)(\hat{X}_{i+1}) & \frac{1}{3}\sum_{i=1}^{3}(\hat{X}_i)(\hat{X}_{i+2}) & \frac{1}{2}\sum_{i=1}^{2}(\hat{X}_i)(\hat{X}_{i+3}) \\ \frac{1}{3}\sum_{i=1}^{3}(\hat{X}_i)(\hat{X}_{i+2}) & \frac{1}{4}\sum_{i=1}^{4}(\hat{X}_i)(\hat{X}_{i+1}) & \frac{1}{5}\sum_{i=1}^{5}(\hat{X}_i)(\hat{X}_i) & \frac{1}{4}\sum_{i=1}^{4}(\hat{X}_i)(\hat{X}_{i+1}) & \frac{1}{3}\sum_{i=1}^{3}(\hat{X}_i)(\hat{X}_{i+2}) \\ \frac{1}{2}\sum_{i=1}^{2}(\hat{X}_i)(\hat{X}_{i+3}) & \frac{1}{3}\sum_{i=1}^{3}(\hat{X}_i)(\hat{X}_{i+2}) & \frac{1}{4}\sum_{i=1}^{4}(\hat{X}_i)(\hat{X}_{i+1}) & \frac{1}{5}\sum_{i=1}^{5}(\hat{X}_i)(\hat{X}_i) & \frac{1}{4}\sum_{i=1}^{4}(\hat{X}_i)(\hat{X}_{i+1}) \\ \frac{1}{1}\sum_{i=1}^{1}(\hat{X}_i)(\hat{X}_{i+4}) & \frac{1}{2}\sum_{i=1}^{2}(\hat{X}_i)(\hat{X}_{i+3}) & \frac{1}{3}\sum_{i=1}^{3}(\hat{X}_i)(\hat{X}_{i+2}) & \frac{1}{4}\sum_{i=1}^{4}(\hat{X}_i)(\hat{X}_{i+1}) & \frac{1}{5}\sum_{i=1}^{5}(\hat{X}_i)(\hat{X}_i) \end{bmatrix} \tag{10}$$

The resulting eigenvalues are 2.53, 1.37, 0.69, 0.55, and −0.15. The negative eigenvalue indicates that the matrix is not positive definite. On the other hand, if Eq. (3) is used for the calculations, the resulting eigenvalues are 1.97, 1.05, 0.83, 0.77, and 0.39. All five eigenvalues are positive, indicating a positive definite matrix. Therefore, only Eq. (3) should be used to calculate the experimental autocorrelation. One may argue that the version of Eq. (3) with $(k-j)$ in the denominator still can be used as long as the resulting experimental values are not used for probabilistic analyses other than to produce a fitted theoretical autocorrelation model. Eq. (10) is always positive definite if it is calculated from such a theoretical model. The authors do not recommend this practice. First, it is a minor effort to replace $(k-j)$ with k in the denominator in exchange for theoretical correctness. Secondly, there are cross-correlations between different soil parameters in addition to spatial autocorrelations in multivariate vector fields. There are no theoretical models to fit cross-correlations to circumvent this problem. In fact, there is a second positive definite problem relating to a cross-correlation matrix constituted by independent evaluation of each pairwise correlation entry (Ching and Phoon 2014). This lack of positive definiteness in some existing methods needs more attention in the literature.

This section reveals that the scales of fluctuation reported in the literature may not be completely accurate. For the method of moments, it is less sensitive to the choice of the autocorrelation function, but it could be less precise and may be based on Eq. (9). For MLE, it can be very sensitive to the choice of the classical one-parameter autocorrelation function, which needs to be identified from actual soil data as well. Nonetheless, a literature survey such as that conducted in the next section is useful if one bears these caveats in mind.

Literature Review of Typical Scales of Fluctuation

Table S1 in the Supplemental Materials summarizes the available data on the horizontal and vertical scale of fluctuation for different soil types collected from published case studies, which can be used as a reference for design when field data are not readily available. When possible, the test types, methods of calculation, and autocorrelation function used to estimate these parameters are reported.

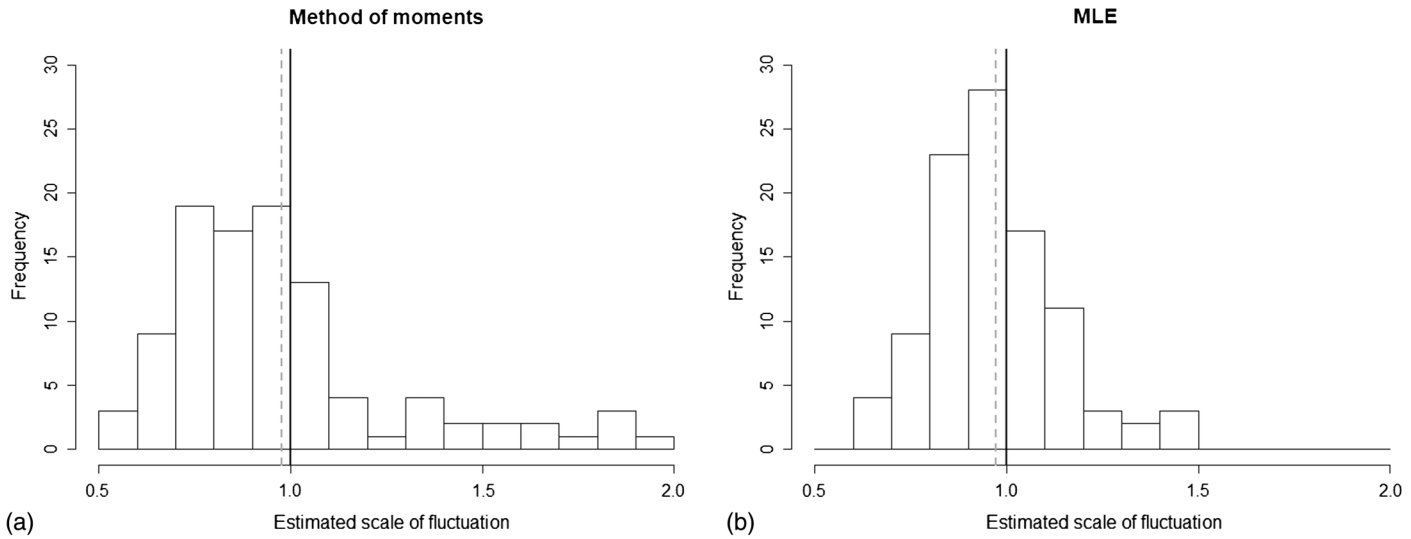

Fig. 6. Histogram of estimated scale of fluctuation values from random field generated with Markovian autocorrelation model: (a) method of moments assuming Markovian autocorrelation; and (b) MLE assuming Markovian autocorrelation. The histograms display 100 values obtained from 20 simulations, sampled in 5 vertical profiles (Fig. 4). Solid vertical line indicates true value of 1 m. Dashed line indicates mean of the histogram [0.98 and 0.97 m, respectively (Table 5)].

Table 7. Five simulated parameter values from CPT sounding, sampled from normal distribution, $N(10, 2^2)$

Depth	Parameter value
0	8.75
$-\delta$	10.37
-2δ	8.33
-3δ	13.19
-4δ	10.66

A description of soil type is useful because the site-specific scale of fluctuation values can be extrapolated to other locations, provided that the soil deposits are of similar geologic formation and environmental history (Phoon and Kulhawy 1999). The same logic can be used for test type. The method of calculation and autocorrelation function are also useful for understanding the assumptions used in these estimations. For most of the cases in Table S1, the vertical scale of fluctuation is available, because site data usually are collected at a much higher spatial resolution in the vertical direction than in the horizontal direction. The original papers reporting these estimations and the papers citing them are included in Table S1. Table S1 is summarized by soil type in Table 8 to provide engineers with a sense of the probable range of values for sensitivity analysis and selection of a prior distribution for Bayesian analysis. Table 8 contains the minimum, maximum, and average values for horizontal and vertical scale of fluctuation for each soil type. As in all literature reviews, it was not possible to ensure that all values are determined based on best practice (appropriate detrending, appropriate choice of ACF, supported by sufficient data, and so forth) and that their quality is uniformly good, despite the best efforts of the authors. Nonetheless, many of the reviewed studies have undergone peer reviews, and the values summarized in this review paper should be regarded as adequate estimates when they are cross-validated by comparable studies. It is prudent to study the original references in more detail for values that depart significantly from this population of comparable studies.

Figs. 7(a and b) provide histogram plots for horizontal and vertical scales of fluctuation, respectively, using the data extracted from Table S1. For cases in which a range was provided, the average was used. With a handful of exceptions, the horizontal scale of fluctuation ranged from nearly 0 to 100 m, with most in the 0–60-m range [Fig. 7(a)]. On the other hand, the vertical scale of fluctuation ranged from nearly 0 to 8 m, with most in the 0–5-m range [Fig. 7(b)]. These ranges are in agreement with ranges presented in literature for horizontal and vertical scales of fluctuation (Phoon and Kulhawy 1999). Additionally, the horizontal scale of fluctuation

Table 8. Summary of scales of fluctuation from literature review (Table S1) by soil type (meters)

	Horizontal θ				Vertical θ			
Soil type	Number averaged	Min	Max	Average	Number averaged	Min	Max	Average
Alluvial	9	1.07	49	14.2	13	0.07	1.1	0.36
Ankara clay	—	—	—	—	4	1	6.2	3.63
Chicago clay	—	—	—	—	2	0.79	1.25	0.91
Clay	9	0.14	163.8	31.9	16	0.05	3.62	1.29
Clay, sand, and silt mix	13	1.2	1,000	201.5	28	0.06	21	1.58
Hangzhou clay	2	40.4	45.4	42.9	4	0.49	0.77	0.63
Marine clay	8	8.37	66	30.9	9	0.11	6.1	1.55
Marine sand	1	15	15	15	5	0.07	7.2	1.43
Offshore soil	1	24.6	66.5	45.6	2	0.48	1.62	1.04
Overconsolidated clay	1	0.14	0.14	0.14	2	0.063	0.255	0.15
Sand	9	1.69	80	24.5	14	0.1	4	1.17
Sensitive clay	—	—	—	—	2	1.1	2.0	1.55
Silt	3	12.7	45.5	33.2	5	0.14	7.19	2.08
Silty clay	7	9.65	45.4	29.8	14	0.095	6.47	1.40
Soft clay	3	22.2	80	47.6	8	0.14	6.2	1.70
Undrained engineered soil	—	—	—	—	22	0.3	2.7	1.42
Water content	9	2.8	22.2	12.9	8	0.05	6.2	1.70

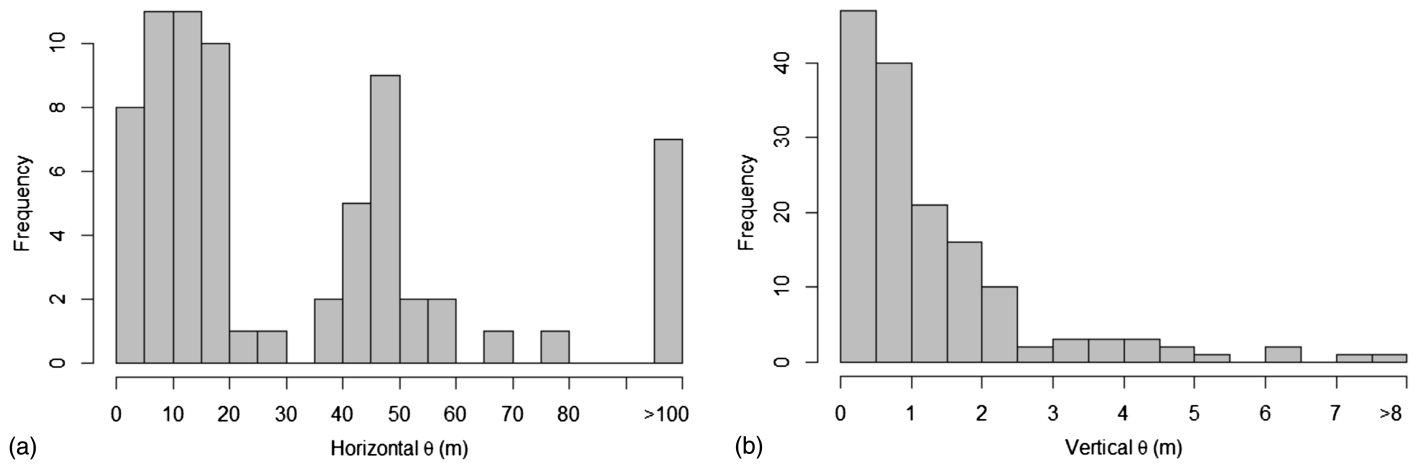

Fig. 7. Histogram plot for scales of fluctuation extracted from Table S1: (a) horizontal; and (b) vertical.

Table 9. Statistical characteristics of cement-admixed soils

References	Test (result)	Scale of fluctuation[a] (m)	
		Vertical	Horizontal
Honjo and Kuroda (1991)	Unconfined compressive test (UCS)	0.8–8.0	—
Hedman and Kuokkanen (2003)	Hand-operated penetrometer test (c_u)	0.38–1.12	0.07–0.33[b]
Navin and Filz (2005)	Unconfined compressive test (UCS)	—	Approximate 24.0
Larsson et al. (2005)[b]	Hand-operated penetrometer test (c_u)	—	Radial: <0.13; and Orthogonal: <0.32[b]
Larsson and Nilsson (2009)	Cone penetration test (tip resistance)	—	1.8–3.6
Al-Naqshabandy et al. (2012)	Cone penetration test (tip resistance)	0.2–0.7	2.0–3.0
Liu et al. (2018)	Centrifuge test (binder concentration[c])	1.0–3.33	Intracolumn[d]: Radial: 0.12D–0.28D Circumferential: 67°–133° Inter-column[d]: 0.12D–0.28D

Source: Liu et al. 2015; Pan et al. 2018, 2019.
[a]Autocorrelation distance used in some studies converted to scale of fluctuation (Vanmarcke 1983) by multiplying by 2.0.
[b]θ within the column cross-section.
[c]Binder concentration is the mass ratio of cement slurry to the whole mixture.
[d]Intracolumn θ refers to variation caused by insufficient mixing; intercolumn θ refers to variation caused by variation of in situ water content.

data fluctuated more from bin to bin than did the vertical data, because more data are available in Table S1 (and generally in the literature) for vertical scale of fluctuation than for horizontal scale of fluctuation.

In addition to Table S1 and the summary in Table 8, Table 9 provides a separate summary of the scale of fluctuation for cement-mixed soils presented by Pan et al. (2018, 2019). The scale of fluctuation for cement-mixed soil is interesting because the spatial variability is a combination of natural variability and variability resulting from the mixing process.

Furthermore, Luo and Bathurst (2018a, b) provided estimates of the scale of fluctuation for the case of reinforced retaining walls. They showed that the vertical scale of fluctuation for these types of structures is equal to or less than the soil compaction length (15–17 cm). In theory, the magnitude of vertical soil strength spatial variability also is important when the vertical scale of fluctuation for anisotropic spatially variable soil strength is less than the reinforcement spacing used in reinforced walls, slopes, and embankments. However, the soils for these systems are engineered materials that must satisfy specified narrow as-built property ranges. This means that spread (uncertainty) in these material properties is small, and hence the influence of spatial variability of soil strength on margins of safety expressed probabilistically is less of a concern. The spatial variability of semiengineered improved soils, whether through mixing with stabilizing agents such as cement or through compaction, is less well studied at present.

Conclusion

This study serves as a practical reference for engineers performing a spatial variability analysis. The purpose of this study was twofold. First, it provided a basic summary of the available methods for estimating the scale of fluctuation and compared them with two simple examples. This revealed the limitations of two popular methods, namely the method of moments and the maximum-likelihood method. The former is less precise, and some studies have adopted a correlation estimator that is not positive definite. The latter can be very sensitive to the choice of the classical one-parameter autocorrelation function. Hence, it should not be assumed, but it should be identified from actual soil data, particularly in conjunction with a more general two-parameter Whittle–Matérn model. More robust estimation methods are needed. The second part of the paper provided a database table of horizontal and vertical scale of fluctuation values in different locations and for different materials, collected from published case studies, as well as a summary of worst-case scales of fluctuation, which can be used as a reference when field data are not available readily. A summary table containing the minimum, maximum, and average value as a function of soil type is particularly useful because it provides engineers with a sense of the probable range of values that can inform a sensitivity analysis and guide the selection of a prior distribution for Bayesian analysis. The values summarized in this review paper should be regarded as adequate estimates when they are cross-validated by comparable studies.

Appendix. Relationship between Whittle–Matérn Model Parameters (x and n) and Scale of Fluctuation (θ)

This appendix derives the equation for the Whittle–Matérn model in Table 2 such that it integrates to θ as in Eq. (2). Consider the following formulation for the Whittle–Matérn model (Hristopulos and Zukovic 2011):

$$\rho(\tau) = \frac{2^{1-\nu}}{\Gamma(\nu)} \cdot \left(\frac{|\tau|}{\xi}\right)^{\nu} K_{\nu}\left(\frac{|\tau|}{\xi}\right) \tag{11}$$

where ξ = scale parameter, which is different from scale of fluctuation θ. Hristopulos and Zukovic (2011) showed that the integral of $\rho(\tau)$ has the following expression:

$$\int_{-\infty}^{\infty} \rho(\tau)d\tau = 2\int_{0}^{\infty} \frac{2^{1-\nu}}{\Gamma(\nu)} \cdot \left(\frac{\tau}{\xi}\right)^{\nu} K_{\nu}\left(\frac{\tau}{\xi}\right)d\tau = 2\pi^{1/2}\left[\frac{\Gamma(\nu+1/2)}{\Gamma(\nu)}\right] \times \xi \tag{12}$$

This integral is exactly θ, hence

$$\theta = 2\pi^{1/2}\left[\frac{\Gamma(\nu+1/2)}{\Gamma(\nu)}\right] \times \xi \tag{13}$$

This suggests that

$$\xi = \frac{\pi^{-1/2}}{2}\left[\frac{\Gamma(\nu)}{\Gamma(\nu+1/2)}\right] \times \theta \tag{14}$$

Inserting Eq. (14) into Eq. (11) obtains

$$\rho(\tau) = \frac{2^{1-\nu}}{\Gamma(\nu)} \cdot \left(\frac{|\tau|}{\frac{\pi^{-1/2}}{2}\left[\frac{\Gamma(\nu)}{\Gamma(\nu+1/2)}\right] \times \theta} \right)^{\nu} K_{\nu}\left(\frac{\sqrt{2\nu} \cdot |\tau|}{\frac{\pi^{-1/2}}{2}\left[\frac{\Gamma(\nu)}{\Gamma(\nu+1/2)}\right] \times \theta} \right)$$
$$= \frac{2}{\Gamma(\nu)} \cdot \left(\frac{\sqrt{\pi} \cdot \Gamma(\nu+1/2) \cdot |\tau|}{\Gamma(\nu) \times \theta} \right)^{\nu} K_{\nu}\left(\frac{\sqrt{\pi} \cdot \Gamma(\nu+1/2) \cdot |\tau|}{\Gamma(\nu) \times \theta} \right) \quad (15)$$

which is the Whittle–Matérn formula in Table 2.

Data Availability Statement

Some or all data, models, or code that support the findings of this study are available from the corresponding author upon reasonable request.

Acknowledgments

The authors thank Professor Bilal Ayyub for his encouragement to prepare this review paper for the ASCE-ASME *Journal of Risk and Uncertainty in Engineering Systems, Part A: Civil Engineering*. The authors also are grateful to Richard J. Bathurst, Nezam Bozorgzadeh, Zijun Cao, Reza Jamshidi Chenari, Jinsong Huang, Shadi Najjar, Qiujing Pan, and Yutao Pan for their invaluable comments and generous assistance in the preparation of this paper. In addition, Dr. Zijun Cao assisted in clarifying the limitations of the method in Fig. 1 and corrected errors in Table 2. Dr. Zijun Cao and Yuxin Lu independently verified the results in Tables 5 and 6. Dr. Yutao Pan provided additional data on cement-mixed soils (Table 9). We thank them for their substantial efforts to improve this paper. The third author extends his appreciation to the Institute for Risk and Reliability, Leibniz University, and the funding from the Alexander von Humboldt Foundation for providing the support to complete this paper. The authors Brigid Cami and Sina Javankhoshdel would like to extend their appreciation to Rocscience for their encouragement in the preparation of this paper.

Supplemental Materials

Table S1 is available online in the ASCE Library (www.ascelibrary.org).

References

Abramowitz, M., and I. Stegun. 1970. *Handbook of mathematical functions*. New York: Dover.

Ahmed, A., and A. H. Soubra. 2014. "Probabilistic analysis at the serviceability limit state of two neighboring strip footings resting on a spatially random soil." *Struct. Saf.* 49 (Jul): 2–9. https://doi.org/10.1016/j.strusafe.2013.08.001.

Ali, A., J. Huang, A. V. Lyamin, S. W. Sloan, D. V. Griffiths, M. J. Cassidy, and J. H. Li. 2014. "Simplified quantitative risk assessment of rainfall-induced landslides modelled by infinite slopes." *Eng. Geol.* 179 (Sep): 102–116. https://doi.org/10.1016/j.enggeo.2014.06.024.

Al-Naqshabandy, M. S., N. Bergman, and S. Larsson. 2012. "Strength variability in lime-cement columns based on CPT data." *Ground Improv.* 165 (1): 15–30. https://doi.org/10.1680/grim.2012.165.1.15.

Anderson, N., N. Croxton, R. Hoover, and P. Sirles. 2008. *Geophysical methods commonly employed for geotechnical site characterization: Transportation research circular E-C130*. Washington, DC: Transportation Research Board.

ArcGIS Desktop Help. 2019. "Understanding a semivariogram: The range, sill, and nugget." Accessed November 16, 2018. http://desktop.arcgis.com/en/arcmap/latest/extensions/geostatistical-analyst/understanding-a-semivariogram-the-range-sill-and-nugget.htm.

Baecher, G. B. 1986. "Geotechnical error analysis." *Transp. Res. Rec.* 1105 (36): 23–31.

Baecher, G. B., and J. T. Christian. 2003. *Reliability and statistics in geotechnical engineering*. West Sussex, UK: Wiley.

Bagińska, I., R. Kupis, and Z. Pochrań. 2012. *Badania sonda statyczna CPTU gruntu nasypowego oraz rodzimego celem analizy stanu i odkształacalności nasypu*. Raport Serii U 18. Wrocław, Poland: Politechnika Wrocławska, Instytut Geotechniki i Hydroechniki.

Bartlett, M. S. 1946. "On the theoretical specification of sampling properties of autocorrelated time-series." Supplement, *J. R. Stat. Soc.* 8 (1): 27–41. https://doi.org/10.2307/2983611.

Breysse, D., H. Niandou, S. Elachachi, and L. Houy. 2005. "A generic approach to soil–structure interaction considering the effects of soil heterogeneity." *Géotechnique* 55 (2): 143–150. https://doi.org/10.1680/geot.2005.55.2.143.

Breysse, D., H. Niandou, S. Elachachi, and L. Houy. 2007. "A generic approach to soil–structure interaction considering the effects of soil heterogeneity." In *Risk and variability in geotechnical engineering*, 117–124. London: Thomas Telford Publishing.

Brockwell, P. J., and R. A. Davis. 1991. *Time series: Theory and methods*. New York: Springer.

Cao, Z., and Y. Wang. 2012. "Bayesian approach for probabilistic site characterization using cone penetration tests." *J. Geotech. Geoenviron. Eng.* 139 (2): 267–276. https://doi.org/10.1061/(ASCE)GT.1943-5606.0000765.

Cassidy, M. J., M. Uzielli, and Y. Tian. 2013. "Probabilistic combined loading failure envelopes of a strip footing on spatially variable soil." *Comput. Geotech.* 49 (Apr): 191–205. https://doi.org/10.1016/j.compgeo.2012.10.008.

Chang, C. C., and D. N. Politis. 2016. "Robust autocorrelation estimation." *J. Comput. Graphical Stat.* 25 (1): 144–166. https://doi.org/10.1080/10618600.2014.969431.

Chiles, J. P., and P. Delfiner. 2009. *Geostatistics: Modeling spatial uncertainty*, 497. New York: Wiley.

Ching, J., Y. G. Hu, and K. K. Phoon. 2016a. "On characterizing spatially variable soil shear strength using spatial average." *Probab. Eng. Mech.* 45 (Jul): 31–43. https://doi.org/10.1016/j.probengmech.2016.02.006.

Ching, J., W. H. Huang, and K. K. Phoon. 2020. "Three-dimensional probabilistic site characterization by sparse Bayesian learning." *J. Eng. Mech.*

Ching, J., S. W. Lee, and K. K. Phoon. 2016b. "Undrained strength for a 3D spatially variable clay column subjected to compression or shear." *Probab. Eng. Mech.* 45 (Jul): 127–139. https://doi.org/10.1016/j.probengmech.2016.03.002.

Ching, J., D. Q. Li, and K. K. Phoon. 2016c. "Statistical characterization of multivariate geotechnical data." Chap. 4 in *Reliability of geotechnical structures in ISO2394*, 89–126. Boca Raton, FL: CRC Press.

Ching, J., and K. K. Phoon. 2013a. "Mobilized shear strength of spatially variable soils under simple stress states." *Struct. Saf.* 41 (Mar): 20–28. https://doi.org/10.1016/j.strusafe.2012.10.001.

Ching, J., and K. K. Phoon. 2013b. "Probability distribution for mobilised shear strengths of spatially variable soils under uniform stress states." *Georisk: Assess. Manage. Risk Eng. Syst. Geohazards* 7 (3): 209–224. https://doi.org/10.1080/17499518.2013.801273.

Ching, J., and K. K. Phoon. 2014. "Correlations among some clay parameters—The multivariate distribution." *Can. Geotech. J.* 51 (6): 686–704. https://doi.org/10.1139/cgj-2013-0353.

Ching, J., and K. K. Phoon. 2017. "Characterizing uncertain site-specific trend function by sparse Bayesian learning." *J. Eng. Mech.* 143 (7): 04017028. https://doi.org/10.1061/(ASCE)EM.1943-7889.0001240.

Ching, J., and K. K. Phoon. 2018. "Impact of autocorrelation function model on the probability of failure." *J. Eng. Mech.* 145 (1): 04018123. https://doi.org/10.1061/(ASCE)EM.1943-7889.0001549.

Ching, J., and K. K. Phoon. 2019. "Constructing site-specific probabilistic transformation model by Bayesian machine learning." *J. Eng. Mech.* 145 (1): 04018126. https://doi.org/10.1061/(ASCE)EM.1943-7889.0001537.

Ching, J., K. K. Phoon, J. L. Beck, and Y. Huang. 2017a. "Identifiability of geotechnical site-specific trend functions." *ASCE-ASME J. Risk Uncertainty Eng. Syst. Part A: Civ. Eng.* 3 (4): 04017021. https://doi.org/10.1061/AJRUA6.0000926.

Ching, J., K. K. Phoon, and Y. K. Pan. 2017b. "On characterizing spatially variable soil Young's modulus using spatial average." *Struct. Saf.* 66 (May): 106–117. https://doi.org/10.1016/j.strusafe.2017.03.001.

Ching, J., K. K. Phoon, A. W. Stuedlein, and M. Jaksa. 2019. "Identification of sample path smoothness in soil spatial variability." *Struct. Saf.* 81 (Nov): 101870. https://doi.org/10.1016/j.strusafe.2019.101870.

Ching, J., K. K. Phoon, and S. P. Sung. 2017c. "Worst case scale of fluctuation in basal heave analysis involving spatially variable clays." *Struct. Saf.* 68 (Sep): 28–42. https://doi.org/10.1016/j.strusafe.2017.05.008.

Ching, J., K. K. Phoon, and S. H. Wu. 2016d. "Impact of statistical uncertainty on geotechnical reliability estimation." *J. Eng. Mech.* 142 (6): 04016027. https://doi.org/10.1061/(ASCE)EM.1943-7889.0001075.

Ching, J., X. W. Tong, and Y. G. Hu. 2016e. "Effective Young's modulus for a spatially variable soil mass subjected to a simple stress state." *Georisk: Assess. Manage. Risk Eng. Syst. Geohazards* 10 (1): 11–26. https://doi.org/10.1080/17499518.2015.1084426.

Ching, J., S. S. Wu, and K. K. Phoon. 2015. "Statistical characterization of random field parameters using frequentist and Bayesian approaches." *Can. Geotech. J.* 53 (2): 285–298. https://doi.org/10.1139/cgj-2015-0094.

Cho, S. E. 2010. "Probabilistic assessment of slope stability that considers the spatial variability of soil properties." *J. Geotech. Geoenviron. Eng.* 136 (7): 975–984. https://doi.org/10.1061/(ASCE)GT.1943-5606.0000309.

Cressie, N. 1992. "Statistics for spatial data." *Terra Nova* 4 (5): 613–617. https://doi.org/10.1111/j.1365-3121.1992.tb00605.x.

DeGroot, D. J., and G. B. Baecher. 1993. "Estimating autocovariance of in-situ soil properties." *J. Geotech. Eng.* 119 (1): 147–166. https://doi.org/10.1061/(ASCE)0733-9410(1993)119:1(147).

Fenton, G. A. 1999. "Estimation for stochastic soil models." *J. Geotech. Geoenviron. Eng.* 125 (6): 470–485. https://doi.org/10.1061/(ASCE)1090-0241(1999)125:6(470).

Fenton, G. A., and D. V. Griffiths. 2003. "Bearing-capacity prediction of spatially random c-φ soils." *Can. Geotech. J.* 40 (1): 54–65. https://doi.org/10.1139/t02-086.

Fenton, G. A., and D. V. Griffiths. 2005. "Three-dimensional probabilistic foundation settlement." *J. Geotech. Geoenviron. Eng.* 131 (2): 232–239. https://doi.org/10.1061/(ASCE)1090-0241(2005)131:2(232).

Fenton, G. A., D. V. Griffiths, and M. B. Williams. 2005. "Reliability of traditional retaining wall design." *Géotechnique* 55 (1): 55–62. https://doi.org/10.1680/geot.2005.55.1.55.

Fenton, G. A., D. V. Griffiths, and M. B. Williams. 2007. "Reliability of traditional retaining wall design." In *Risk and variability in geotechnical engineering*, 165–172. London: Thomas Telford.

Griffiths, D. V., and G. A. Fenton. 1993. "Seepage beneath water retaining structures founded on spatially random soil." *Géotechnique* 43 (4): 577–587. https://doi.org/10.1680/geot.1993.43.4.577.

Griffiths, D. V., G. A. Fenton, and N. Manoharan. 2006. "Undrained bearing capacity of two-strip footings on spatially random soil." *Int. J. Geomech.* 6 (6): 421–427. https://doi.org/10.1061/(ASCE)1532-3641(2006)6:6(421).

Griffiths, D. V., J. Huang, and G. A. Fenton. 2009. "Influence of spatial variability on slope reliability using 2-D random fields." *J. Geotech. Geoenviron. Eng.* 135 (10): 1367–1378. https://doi.org/10.1061/(ASCE)GT.1943-5606.0000099.

Hedman, P., and M. Kuokkanen. 2003. "Strength distribution in lime-cement columns—Field tests at Strängnäs." [In Swedish.] M.Sc. thesis, Royal Institute of Technology.

Hicks, M. A. 2012. "An explanation of characteristic values of soil properties in Eurocode 7." In Vol. 1 of *Modern geotechnical design codes of practice: Implementation, application and development*, 36. Amsterdam, Netherlands: IOS Press.

Hicks, M. A., and J. D. Nuttall. 2012. "Influence of soil heterogeneity on geotechnical performance and uncertainty: A stochastic view on EC7." In *Proc., 10th Int. Probabilistic Workshop*, 215–227. Stuttgart, Germany: Universität Stuttgart.

Hicks, M. A., and C. Onisiphorou. 2005. "Stochastic evaluation of static liquefaction in a predominantly dilative sand fill." *Géotechnique* 55 (2): 123–133. https://doi.org/10.1680/geot.2005.55.2.123.

Hicks, M. A., and W. A. Spencer. 2010. "Influence of heterogeneity on the reliability and failure of a long 3D slope." *Comput. Geotech.* 37 (7–8): 948–955. https://doi.org/10.1016/j.compgeo.2010.08.001.

Hicks, M. A., D. Varkey, A. P. van den Eijnden, T. de Gast, and P. J. Vardon. 2019. "On characteristic values and the reliability-based assessment of dykes." *Georisk: Assess. Manage. Risk Eng. Syst. Geohazards* 13 (4): 313–319. https://doi.org/10.1080/17499518.2019.1652918.

Honjo, Y., and K. Kuroda. 1991. "A new look at fluctuating geotechnical data for reliability design." *Soils Found.* 31 (1): 110–120. https://doi.org/10.3208/sandf1972.31.110.

Hristopulos, D. T., and M. Žukovič. 2011. "Relationships between correlation lengths and integral scales for covariance models with more than two parameters." *Stochastic Environ. Res. Risk Assess.* 25 (1): 11–19. https://doi.org/10.1007/s00477-010-0407-y.

Hu, Y. G., and J. Ching. 2015. "Impact of spatial variability in soil shear strength on active lateral forces." *Struct. Saf.* 52 (Jan): 121–131. https://doi.org/10.1016/j.strusafe.2014.09.004.

Huang, J., A. V. Lyamin, D. V. Griffiths, K. Krabbenhoft, and S. W. Sloan. 2013. "Quantitative risk assessment of landslide by limit analysis and random fields." *Comput. Geotech.* 53 (Sep): 60–67. https://doi.org/10.1016/j.compgeo.2013.04.009.

Huang, J. S., D. V. Griffiths, and G. A. Fenton. 2010. "System reliability of slopes by RFEM." *Soils Found.* 50 (3): 343–353. https://doi.org/10.3208/sandf.50.343.

Jaksa, M. B., J. S. Goldsworthy, G. A. Fenton, W. S. Kaggwa, D. V. Griffiths, Y. L. Kuo, and H. G. Poulos. 2005. "Towards reliable and effective site investigations." *Géotechnique* 55 (2): 109–121. https://doi.org/10.1680/geot.2005.55.2.109.

Javankhoshdel, S. 2016. "Reliability analysis of simple slopes and soil-structures with linear limit states." Ph.D. dissertation, Dept. of Civil Engineering, Queen's Univ.

Javankhoshdel, S., and R. J. Bathurst. 2014. "Simplified probabilistic slope stability design charts for cohesive and (c-φ) soils." *Can. Geotech. J.* 51 (9): 1033–1045. https://doi.org/10.1139/cgj-2013-0385.

Javankhoshdel, S., N. Luo, and R. J. Bathurst. 2017. "Probabilistic analysis of simple slopes with cohesive soil strength using RLEM and RFEM." *Georisk: Assess. Manage. Risk Eng. Syst. Geohazards* 11 (3): 231–246. https://doi.org/10.1080/17499518.2016.1235712.

Jha, S. K., and J. Ching. 2013. "Simplified reliability method for spatially variable undrained engineered slopes." *Soils Found.* 53 (5): 708–719. https://doi.org/10.1016/j.sandf.2013.08.008.

Jiang, S. H., and J. Huang. 2018. "Modeling of non-stationary random field of undrained shear strength of soil for slope reliability analysis." *Soils Found.* 58 (1): 185–198. https://doi.org/10.1016/j.sandf.2017.11.006.

Jiang, S. H., D. Q. Li, L. M. Zhang, and C. B. Zhou. 2014. "Slope reliability analysis considering spatially variable shear strength parameters using a non-intrusive stochastic finite element method." *Eng. Geol.* 168 (Jan): 120–128. https://doi.org/10.1016/j.enggeo.2013.11.006.

Krige, D. G. 1951. "A statistical approach to some basic mine valuation problems on the Witwatersrand." *J. South Afr. Inst. Min. Metall.* 52 (6): 119–139.

Krige, D. G. 1966. "Two-dimensional weighted moving average trend surfaces for ore-evaluation." *J. South Afr. Inst. Min. Metall.* 66 (Mar): 13–38.

Lacasse, S., and F. Nadim. 1996. "Uncertainties in characterising soil properties." In *Uncertainty in the geologic environment: From theory to practice*, 49–75. Reston, VA: ASCE.

Larsson, S., and A. Nilsson. 2009. "Horizontal strength variability in lime-cement columns." In *Proc., Int. Symp. on Deep Mixing and Admixture Stabilizaton*, edited by M. Kitazume, M. Terashi, S. Tokunaga, and N. Yasuoka, 629–634. Tokyo: Sanwa Company.

Larsson, S., H. Stille, and L. Olsson. 2005. "On horizontal variability in lime-cement columns in deep mixing." *Géotechnique* 55 (1): 33–44. https://doi.org/10.1680/geot.2005.55.1.33.

Le, T. M. H. 2014. "Reliability of heterogeneous slopes with cross-correlated shear strength parameters." *Assess. Manage. Risk Eng. Syst. Geohazards* 8 (4): 250–257.

Li, D. Q., S. H. Jiang, Z. J. Cao, W. Zhou, C. B. Zhou, and L. M. Zhang. 2015a. "A multiple response-surface method for slope reliability analysis considering spatial variability of soil properties." *Eng. Geol.* 187 (Mar): 60–72. https://doi.org/10.1016/j.enggeo.2014.12.003.

Li, D. Q., T. Xiao, L. M. Zhang, and Z. J. Cao. 2019. "Stepwise covariance matrix decomposition for efficient simulation of multivariate large-scale three-dimensional random fields." *Appl. Math. Modell.* 68 (Apr): 169–181. https://doi.org/10.1016/j.apm.2018.11.011.

Li, J. H., Y. Zhou, L. L. Zhang, Y. Tian, M. J. Cassidy, and L. M. Zhang. 2016. "Random finite element method for spudcan foundations in spatially variable soils." *Eng. Geol.* 205 (Apr): 146–155. https://doi.org/10.1016/j.enggeo.2015.12.019.

Liu, W. F., and Y. F. Leung. 2017. "Characterising three-dimensional anisotropic spatial correlation of soil properties through in situ test results." *Géotechnique* 68 (9): 805–819. https://doi.org/10.1680/jgeot.16.P.336.

Liu, W. F., Y. F. Leung, and M. K. Lo. 2016. "Integrated framework for characterization of spatial variability of geological profiles." *Can. Geotech. J.* 54 (1): 47–58. https://doi.org/10.1139/cgj-2016-0189.

Liu, Y., L. Q. He, Y. J. Jiang, M. M. Sun, E. J. Chen, and F. H. Lee. 2018. "Effect of in situ water content variation on the spatial variation of strength of deep cement-mixed clay." *Géotechnique* 69 (5): 391–405. https://doi.org/10.1680/jgeot.17.P.149.

Liu, Y., F. H. Lee, S. T. Quek, E. J. Chen, and J. T. Yi. 2015. "Effect of spatial variation of strength and modulus on the lateral compression response of cement-admixed clay slab." *Géotechnique* 65 (10): 851–865. https://doi.org/10.1680/jgeot.14.P.254.

Lloret-Cabot, M. F. G. A., G. A. Fenton, and M. A. Hicks. 2014. "On the estimation of scale of fluctuation in geostatistics." *Georisk: Assess. Manage. Risk Eng. Syst. Geohazards* 8 (2): 129–140. https://doi.org/10.1080/17499518.2013.871189.

Lumb, P. 1975. "Spatial variability of soil properties." In *Proc., 2nd Int. Conf. on Applications of Statistics and Probability to Soil and Structural Engineering*, 397–421. Effen, Germany: Deutche Gesellschaft fuer Erd-und.

Luo, N., and R. J. Bathurst. 2018a. "Deterministic and random FEM analysis of full-scale unreinforced and reinforced embankments." *Geosynthetics Int.* 25 (2): 164–179. https://doi.org/10.1680/jgein.17.00040.

Luo, N., and R. J. Bathurst. 2018b. "Probabilistic analysis of reinforced slopes using RFEM and considering spatial variability of frictional soil properties due to compaction." *Georisk: Assess. Manage. Risk Eng. Syst. Geohazards* 12 (2): 87–108. https://doi.org/10.1080/17499518.2017.1362443.

Luo, N., R. J. Bathurst, and S. Javankhoshdel. 2016. "Probabilistic stability analysis of simple reinforced slopes by finite element method." *Comput. Geotech.* 77 (Jul): 45–55. https://doi.org/10.1016/j.compgeo.2016.04.001.

Mariethoz, G., and J. Caers. 2014. *Multiple-point geostatistics: Stochastic modeling with training images*. New York: Wiley.

Matheron, G. 1963. "Principles of geostatistics." *Econ. Geol.* 58 (8): 1246–1266. https://doi.org/10.2113/gsecongeo.58.8.1246.

McCuen, R. H., M. S. Aggour, and B. M. Ayyub. 1988. "Spacing for accuracy in ultrasonic testing for bridge timber piles." *J. Struct. Eng.* 114 (12): 2652–2668. https://doi.org/10.1061/(ASCE)0733-9445(1988)114:12(2652).

Montoya-Noguera, S., T. Zhao, Y. Hu, Y. Wang, and K. K. Phoon. 2019. "Simulation of non-stationary non-Gaussian random fields from sparse measurements using Bayesian compressive sampling and Karhunen-Loève expansion." *Struct. Saf.* 79 (Jul): 66–79. https://doi.org/10.1016/j.strusafe.2019.03.006.

Navin, M. P., and G. M. Filz. 2005. "Statistical analysis of strength data from ground improved with DMM columns." In *Proc., Int. Conf. on Deep Mixing Best Practice and Recent Advances, Deep Mixing '05*. Linköping, Sweden: Swedish Geotechnical Institute.

Paiboon, J., D. V. Griffiths, J. Huang, and G. A. Fenton. 2013. "Numerical analysis of effective elastic properties of geomaterials containing voids using 3D random fields and finite elements." *Int. J. Solids Struct.* 50 (20–21): 3233–3241. https://doi.org/10.1016/j.ijsolstr.2013.05.031.

Pan, Y., Y. Liu, H. Xiao, F. H. Lee, and K. K. Phoon. 2018. "Effect of spatial variability on short-and long-term behaviour of axially-loaded cement-admixed marine clay column." *Comput. Geotech.* 94 (Feb): 150–168. https://doi.org/10.1016/j.compgeo.2017.09.006.

Pan, Y., K. Yao, K. K. Phoon, and F. H. Lee. 2019. "Analysis of tunnelling through spatially-variable improved surrounding—A simplified approach." *Tunnelling Underground Space Technol.* 93 (Nov): 103102. https://doi.org/10.1016/j.tust.2019.103102.

Papaioannou, I., and D. Straub. 2017. "Learning soil parameters and updating geotechnical reliability estimates under spatial variability—Theory and application to shallow foundation." *Georisk: Assess. Manage. Risk Eng. Syst. Geohazards* 11 (1): 116–128. https://doi.org/10.1080/17499518.2016.1250280.

Phoon, K. K. 2017. "Role of reliability calculations in geotechnical design." *Georisk: Assess. Manage. Risk Eng. Syst. Geohazards* 11 (1): 4–21. https://doi.org/10.1080/17499518.2016.1265653.

Phoon, K. K., and G. A. Fenton. 2004. "Estimating sample autocorrelation functions using bootstrap." In *Proc., 9th ASCE Specialty Conf. on Probabilistic Mechanics and Structural Reliability*, 26–28. Reston, VA: ASCE.

Phoon, K. K., and F. H. Kulhawy. 1999. "Characterization of geotechnical variability." *Can. Geotech. J.* 36 (4): 612–624. https://doi.org/10.1139/t99-038.

Phoon, K. K., and Y. Wang. 2019. "Chicken (method) and egg (data)—Which comes first?" In *Proc., Int. Symp. on Reliability of Multi-disciplinary Engineering Systems under Uncertainty (ISRMES2019)*. Da'an, Taipei: Ministry of Education and Ministry of Science and Technology.

Pieczyńska-Kozłowska, J. M. 2015. "Comparison between two methods for estimating the vertical scale of fluctuation for modeling random geotechnical problems." *Stud. Geotech. et Mech.* 37 (4): 95–103. https://doi.org/10.1515/sgem-2015-0049.

Priestley, M. B. 1981. *Spectral analysis and time series*. New York: Academic Press.

Rasmussen, C. E., and C. K. I. Williams. 2006. *Gaussian processes for machine learning*. Cambridge, MA: MIT Press.

Rice, S. O. 1944. "Mathematical analysis of random noise." *Bell Syst. Tech. J.* 23 (3): 282–332. https://doi.org/10.1002/j.1538-7305.1944.tb00874.x.

Shahmalekpoor, P., R. Jamshidi Chenari, and S. Javankhoshdel. 2020. "Discussion of 'Probabilistic seismic slope stability analysis and design'." *Can. Geotech. J.* 57 (7): 1103–1108. https://doi.org/10.1139/cgj-2019-0386.

Soubra, A. H., and D. Y. A. Massih. 2010. "Probabilistic analysis and design at the ultimate limit state of obliquely loaded strip footings." *Géotechnique* 60 (4): 275–285. https://doi.org/10.1680/geot.7.00031.

Soubra, A. H., Y. A. Massih, and M. Kalfa. 2008. "Bearing capacity of foundations resting on a spatially random soil." In *Proc., GeoCongress 2008: Geosustainability and Geohazard Mitigation (ASCEGSP 178)*, 66–73. Reston, VA: ASCE. https://doi.org/10.1061/9780784409718.

Spry, M. J., F. H. Kulhawy, and M. D. Grigoriu. 1988. *Reliability-based foundation design for transmission line structures: Geotechnical site characterization strategy*. Rep. No. EL-5507. Palo Alto, CA: Electric Power Research Institute.

Stuedlein, A. W., and T. Bong. 2017. "Effect of spatial variability on static and liquefaction-induced differential settlements." In *Proc., Geo-Risk 2017*, 31–51. Reston, VA: ASCE.

Stuedlein, A. W., S. L. Kramer, P. Arduino, and R. D. Holtz. 2012. "Reliability of spread footing performance in desiccated clay." *J. Geotech. Geoenviron. Eng.* 138 (11): 1314–1325. https://doi.org/10.1061/(ASCE)GT.1943-5606.0000706.

Tang, W. H. 1979. "Probabilistic evaluation of penetration resistances." *J. Geotech. Geoenviron. Eng. Div.* 105 (10): 1173–1191.

Tian, M., D. Q. Li, Z. J. Cao, K. K. Phoon, and Y. Wang. 2016. "Bayesian identification of random field model using indirect test data." *Eng. Geol.* 210 (Aug): 197–211. https://doi.org/10.1016/j.enggeo.2016.05.013.

Uzielli, M., G. Vannucchi, and K. K. Phoon. 2005. "Random field characterisation of stress-normalised cone penetration testing parameters." *Géotechnique* 55 (1): 3–20. https://doi.org/10.1680/geot.2005.55.1.3.

Vanmarcke, E. H. 1977. "Probabilistic modeling of soil profiles." *J. Geotech. Eng. Div.* 103 (11): 1227–1246.

Vanmarcke, E. H. 1983. *Random fields: Analysis and synthesis*. Cambridge, MA: MIT Press.

Vessia, G., C. Cherubini, J. Pieczyńska, and W. Puła. 2009. "Application of random finite element method to bearing capacity design of strip footing." *J. Geoeng.* 4 (3): 103–111.

Wackernagel, H. 2003. *Multivariate geostatistics: An introduction with applications*. Berlin: Springer.

Wang, Y., S. K. Au, and Z. Cao. 2010. "Bayesian approach for probabilistic characterization of sand friction angles." *Eng. Geol.* 114 (3–4): 354–363. https://doi.org/10.1016/j.enggeo.2010.05.013.

Wang, Y., and T. Zhao. 2016. "Interpretation of soil property profile from limited measurement data: A compressive sampling perspective." *Can. Geotech. J.* 53 (9): 1547–1559. https://doi.org/10.1139/cgj-2015-0545.

Wang, Y., and T. Zhao. 2017. "Statistical interpretation of soil property profiles from sparse data using Bayesian compressive sampling." *Géotechnique* 67 (6): 523–536. https://doi.org/10.1680/jgeot.16.P.143.

Wang, Y., T. Zhao, and Z. Cao. 2019a. "Bayesian perspective on ground property variability for geotechnical practice." In *Proc., 7th Int. Symp. on Geotechnical Safety and Risk (ISGSR 2019)*. Singapore: Research Publishing.

Wang, Y., T. Zhao, Y. Hu, and K. K. Phoon. 2019b. "Simulation of random fields with trend from sparse measurements without de-trending." *J. Eng. Mech.* 145 (2): 04018130. https://doi.org/10.1061/(ASCE)EM.1943-7889.0001560.

Wang, Y., T. Zhao, and K. K. Phoon. 2017. "Direct simulation of random field samples from sparsely measured geotechnical data with consideration of uncertainty in interpretation." *Can. Geotech. J.* 55 (6): 862–880. https://doi.org/10.1139/cgj-2017-0254.

White, G. J., and B. M. Ayyub. 1990. "Semivariogram and kriging analysis in developing sampling strategies (corrosion)." In *Proc., 1st Int. Symp. on Uncertainty Modeling and Analysis*, 360–365. New York: IEEE. https://doi.org/10.1109/ISUMA.1990.151279.

Xiao, T., D. Q. Li, Z. J. Cao, S. K. Au, and K. K. Phoon. 2016. "Three-dimensional slope reliability and risk assessment using auxiliary random finite element method." *Comput. Geotech.* 79 (Oct): 146–158. https://doi.org/10.1016/j.compgeo.2016.05.024.

Xiao, T., D. Q. Li, Z. J. Cao, and L. M. Zhang. 2018. "CPT-based probabilistic characterization of three-dimensional spatial variability using MLE." *J. Geotech. Geoenviron. Eng.* 144 (5): 04018023. https://doi.org/10.1061/(ASCE)GT.1943-5606.0001875.

Xiao, T., D. Q. Li, Z. J. Cao, and L. M. Zhang. 2019. "Probabilistic characterization of 3-D spatial variability of soils: Methodology and strategy." In *Proc., 13th Int. Conf. on Applications of Statistics and Probability in Civil Engineering*. Vancouver, BC, Canada: International Civil Engineering Risk and Reliability Association.

Zhang, L. M., and S. M. Dasaka. 2010. "Uncertainties in geologic profiles versus variability in pile founding depth." *J. Geotech. Geoenviron. Eng.* 136 (11): 1475–1488. https://doi.org/10.1061/(ASCE)GT.1943-5606.0000364.

Zhao, T., and Y. Wang. 2018. "Simulation of cross-correlated random field samples from sparse measurements using Bayesian compressive sensing." *Mech. Syst. Sig. Process.* 112 (Nov): 384–400. https://doi.org/10.1016/j.ymssp.2018.04.042.

Zhu, D., D. V. Griffiths, and G. A. Fenton. 2018. "Worst-case spatial correlation length in probabilistic slope stability analysis." *Géotechnique* 69 (1): 85–88. https://doi.org/10.1680/jgeot.17.T.050.

Zhu, Y. X., S. Zheng, Z. J. Cao, and D. Q. Li. 2019. "Revisiting the relationship between scale of fluctuation and mean cross distance." In *Proc., 13th Int. Conf. on Applications of Statistics and Probability in Civil Engineering*. Seoul: Seoul Metropolitan Government.